GRADUATE SCHOOL
EAST TENNESSEE STATE UNIVERSITY

East Tennessee State University
Digital Commons @ East Tennessee State University

Electronic Theses and Dissertations

Student Works

8-2022

Cyclic di-GMP Regulates Motility, Biofilm Formation, and Desiccation Tolerance in Acinetobacter baumannii

Garrett Reynolds
East Tennessee State University

Follow this and additional works at: https://dc.etsu.edu/etd

 Part of the Bacteriology Commons, Medical Microbiology Commons, and the Pathogenic Microbiology Commons

Recommended Citation

Reynolds, Garrett, "Cyclic di-GMP Regulates Motility, Biofilm Formation, and Desiccation Tolerance in Acinetobacter baumannii" (2022). *Electronic Theses and Dissertations.* Paper 4116. https://dc.etsu.edu/etd/4116

This Thesis - embargo is brought to you for free and open access by the Student Works at Digital Commons @ East Tennessee State University. It has been accepted for inclusion in Electronic Theses and Dissertations by an authorized administrator of Digital Commons @ East Tennessee State University. For more information, please contact digilib@etsu.edu.

Cyclic di-GMP Regulates Motility, Biofilm Formation, and Desiccation Tolerance in *Acinetobacter baumannii*

A thesis

presented to

the faculty of the Department of Health Sciences

East Tennessee State University

In partial fulfillment

of the requirements for the degree

Master of Science in Biology, Microbiology

---

by

Garrett Reynolds

August 2022

Dr. Erik Petersen

Dr. Bert Lampson

Dr. Christopher Pritchett

Keywords: AB5075, c-di-GMP, CME, DGC, PDE, persistence

ABSTRACT

Cyclic di-GMP Regulates Motility, Biofilm Formation, and

Desiccation Tolerance in *Acinetobacter baumannii*

by

Garrett Reynolds

Acinetobacter baumannii is an increasingly multidrug-resistant pathogen contributing to hospital-acquired infections necessitating the discovery of novel treatments. A bacterial second messenger, cyclic diguanosine monophosphate (cyclic di-GMP), can regulate various persistence factors that are potentially advantageous for survival in hospital environments. Cyclic di-GMP–modulating enzymes and cyclic di-GMP–binding effectors predictively are encoded in the *Acinetobacter baumannii* genome. I hypothesized that cyclic di-GMP controls motility, biofilm formation, and desiccation tolerance in *Acinetobacter baumannii*. Disrupting cyclic di-GMP–modulating enzymes or cyclic di-GMP–binding effectors should alter the regulatory effectiveness of these phenotypes. I tested the multidrug-resistant isolate *Acinetobacter baumannii* strain AB5075 and identified several transposon mutants that altered twitching motility, biofilm formation, and desiccation tolerance; these results suggest that cyclic di-GMP plays a role during these three responses in *Acinetobacter baumannii* AB5075. Inhibiting these cyclic di-GMP signaling pathways could produce novel mechanisms to combat this pathogen in the hospital environment.

© 2022 by Garrett Reynolds

All Rights Reserved

DEDICATION

I dedicate this work to my friends and family for their patience as I continue my academic career: my partner, Carrie “Kat” Matherly, for pushing me, reading my thesis, and letting me know whether it’s worthy, garbage, or worthy garbage; my parents, John and TeriAnn Reynolds, for raising me, giving me life, and giving me consciousness—even if I didn’t ask to be born, I value how you’ve raised me and what you’ve given me; Dr. Robert Pack, for being a mentor to me since high school and rooting for me ’til this day; my grandparents, Dick and Judy Rowe, for providing me financial assistance in my academics; my brother, Matthew Reynolds, for keeping me sane throughout the 23 (and three-fourths!) years of my life; and all my friends including Cannon Pack, Gabriel Davis, and everybody else who has helped me make it through my academic career, unscathed.

And most importantly, I dedicate this work to the United States of America.

ACKNOWLEDGEMENTS

First and foremost, I would like to thank my mentor, Dr. Erik Petersen, for giving me the privilege of working in his research lab and spending so much of his time teaching me. I would also like to express my gratitude to my committee members, Dr. Bert Lampson and Dr. Christopher Pritchett for providing valuable critiques and necessary feedback for this thesis. I additionally would like to acknowledge Dr. Melissa Altura and Dr. Sean Fox for their aid in pedagogical instruction. Gabriel Smith and Gabrielle Shipstone provided much-needed help as undergraduate researchers, assisting me with the motility and desiccation assays. I also thank everybody else in Dr. Petersen's lab who had a direct or indirect impact on my project including Jake Schultz, Joey Headrick, Deeba Mohseni, Zoe Tolzmann, Saahil Narwani, Lexie Pulliam, Abdulafiz Musa, and Andrew Robinson.

TABLE OF CONTENTS

LIST OF FIGURES

LIST OF ABBREVIATIONS

AB5075	*Acinetobacter baumannii* strain AB5075
CBE	Cyclic-di-GMP–binding effector
C-di-GMP	Cyclic di-GMP or bis-(3'-5')-cyclic dimeric guanosine monophosphate
CME	C-di-GMP–modulating enzyme
DCE	Dual domain (both DGC and PDE) c-di-GMP–modulating enzyme
DGC	Diguanylate cyclase
IPTG	Isopropyl β-D-1-thiogalactopyranoside
LB	Luria broth
PDE	C-di-GMP–specific phosphodiesterase
pEV	Empty vector, particularly the pMMB-RIF control vector denoted as "pEV"
WT	A wild type. A wild-type strain

CHAPTER 1. INTRODUCTION

ESKAPE Pathogens

ESKAPE pathogens comprise many multidrug-resistant bacterial strains that cause nosocomial infections in hospitals. The acronym encompasses six pathogens: *Enterococcus faecium*, *Staphylococcus aureus*, *Klebsiella pneumoniae*, *Acinetobacter baumannii*, *Pseudomonas aeruginosa*, and *Enterobacter* spp (1, 2). Many nosocomial strains thrive in hospitals because of their multidrug resistance. A tertiary care teaching hospital in Monterey, Mexico, observed the resistance of *A. baumannii* to meropenem increase from 59 % to 75.3 % within two years (3). Separately, a Hungarian tertiary care teaching hospital found that 55.2 % of isolated *A. baumannii* strains were resistant to meropenems which is much higher than the European average of 31.9 % per the 2018 EARS-NET surveillance system report (4). ESKAPE pathogens share similar mechanisms of antimicrobial resistance, such as drug inactivation, modifying the drug binding site, reducing intracellular drug accumulation by employing efflux pumps/porin loss, and protective biofilm formation (2). Investigating these antimicrobial resistance mechanisms (e.g., biofilm formation) may help researchers avoid these responses when developing disinfectants and antimicrobials.

Conventional antimicrobial treatments are not an effective long-term strategy against bacterial biofilms on abiotic surfaces (5-7). Many biofilm infections are present on medical implant surfaces. Consequently, phagocytes and polymorphonuclear leukocytes are downregulated when in the presence of a foreign body, providing an ideal site for bacterial biofilms to propagate (8, 9). The successful infection is a direct

cause due to a weaker immune response near the site of implants and a safer place for pathogens to thrive. Thus, patients may need to replace their implanted devices and undergo antibiotic treatments to remove the infected surface.

Targeting the pathogens' natural physiological processes (e.g., biofilm formation, motility, et cetera) is a promising aim to diminish their ability to adhere to abiotic surfaces, such as medical equipment or hospital surfaces. One crucial step to finding potential drug and disinfectant targets is understanding more about the physiology of ESKAPE pathogens, providing avenues toward solving the multidrug resistance problem that healthcare facilities face.

Acinetobacter baumannii

Acinetobacter is an aerobic Gram-negative coccobacillus that is not conventionally motile due to the absence of flagella. This opportunistic pathogen is known for its excessive persistence in healthcare facilities and resistance to many antibiotics (e.g., carbapenems), alerting the critical necessity to discover more antimicrobial drugs (10). The most common pathogen for *Acinetobacter* hospital-acquired infections is *A. baumannii* which was responsible for 1.6 % to 6.2 % of total hospital-acquired infections in several surveys (11-13). Because the pathogen's incidence rate in hospitals is ever-increasing, understanding the persistence mechanisms on surfaces will help locate key antimicrobial targets.

Multidrug-resistant *A. baumannii* are often resistant to cephalosporins, fluoroquinolones, and aminoglycosides; so physicians must resort to treating patients with drugs that are becoming less effective against *A. baumannii*, such as polymyxins

and carbapenems (14). In 2017, the World Health Organization listed carbapenem-resistant *A. baumannii* as a critical priority antibiotic-resistant pathogen (10). Particularly, *A. baumannii* strain AB5075 is a recent multidrug-resistant isolate that is a great candidate for studying the persistence of *A. baumannii* because of its phenomenal ability to survive hazardous environments (15). AB5075 is hypervirulent in animal models and prone to genetic manipulation due to its susceptibility to tetracycline, hygromycin, and rifampicin (16). AB5075 also shows high levels of phase variation in colony morphotype, alternating between opaque and translucent colonies. Opaque variants are more common in a motile and virulent state, yet the translucent counterparts are more sessile (17). Moreover, *A. baumannii* incidence has increased in the last decade (18, 19). Since AB5075 is an emerging *A. baumannii* pathogenic hospital strain, the strain should prove a commendable candidate for better understanding the persistence of *Acinetobacter*.

Persistence Factors

Motility

Since *Acinetobacter* lack flagella, the genus is designated as non-motile. In some However, *A. baumannii* encodes a type IV pilus that permits twitching motility in some strains (e.g., AB5075) when the bacterium extends, tethers, and retracts type IV pili to *twitch* across a surface such as plastic. First discovered in the 1970s in *Pseudomonas aeruginosa*, type IV pili contain a major pilin protein (e.g., PilA) and are responsible for elongation and retraction (20-22). Bacteria capable of twitching motility do so entirely independent of flagella (23); the downside is that the bacterium must grapple onto a

hard surface to pull itself forward rather than rotate a helical propeller without needing a surface. In addition to motility, pili can also play a role in adhering to biotic and abiotic surfaces (24-27). The Csu pilus, an adhesive D-mannose-sensitive type I pilus, can accomplish this surface adhesion (28, 29). A bacterium can adhere to and colonize a hard surface using Csu pili, so these pili are not used for motility but for surface adhesion. A bacterium that can grapple onto hard surfaces can expediently colonize onto polyethylene (28), a common polymer used in implanted medical device plastics.

Biofilm Formation

A. baumannii can also form extracellular polymers and clump together in communal structures known as biofilms. In nature, biofilms harbor a diverse crowd of microbes that encase themselves in polysaccharides, exudates, and detritus (30). These extracellular components act as physical barriers that can stop deadly chemicals and allow many bacteria to successfully infect a host (31, 32). Biofilms provide a further barrier that help populations of bacteria colonize hazardous areas to which they cannot easily attach. Bacteria can also utilize biofilms to persist in patients afflicted by chronic infections such as cystic fibrosis, tuberculosis, and sinusitis (33), complicated by the fact that antibiotics are more capable of harming planktonic bacteria compared to biofilm-encased ones (34). Many *A. baumannii* genes may regulate the production of extracellular components for bacterial biofilm formation. One example is *pgaA* with homology to that which has been reported as required for an optimal biofilm in *Escherichia coli*, where *pgaA* binds to the outer membrane exporter for the biofilm adhesin polysaccharide, poly-β-1,6-*N*-acetyl-D-glucosamine (35, 36). Another potential factor in optimal biofilm production is the *algC* gene which codes for

phosphomannomutase, an enzyme that converts mannose-6-phosphate to mannose-1-phosphate (37) that is necessary for the overall synthesis of alginate. Previous studies indicate that alginate exopolysaccharide protects a cell from antimicrobials and a host's immune response within a biofilm (38, 39). The *algC* gene is positively regulated by AlgR (40) and expressed under various conditions such as dehydration or oxidative stress (41). Investigating the regulatory mechanisms behind *A. baumannii* biofilm formation can provide much-needed information on these persistence factors for the eventual development of compounds that treat both surface-associated and *in vivo* biofilms.

Desiccation Tolerance

Another powerful adaptation for *A. baumannii* is to survive on dry surfaces for an extended amount of time; accordingly, the pathogen can persist in healthcare environments outside of liquid solutions, remain viable, and infect once resuspended. Currently, only a few factors have been contributed to desiccation tolerance such as a two-component response regulator, BfmR, and a monofunctional catalase system, KatE, mediate tolerance during desiccation; during that study, AB5075 remained viable on a polystyrene surface for 90 days (15). AB5075 has shown to be much better at resisting dry environments down to 2 % relative humidity than *P. aeruginosa* PAO1, *E. coli* W3110, *A. baumannii* 17978, and *A. baumannii* ATCC® 19606™ during six days (42). Many recent hospital isolates of *A. baumannii* (i.e., AB5075 from 2007 & AB09-003 from 2009) have been more tolerant to dryness compared to older isolates according to the findings of these studies (15, 42, 43).

Bis-(3’-5’)-cyclic Dimeric Guanosine Monophosphate

Bis-(3’-5’)-cyclic dimeric guanosine monophosphate (c-di-GMP) is a bacterial second messenger that controls many physiological states in response to environmental stimuli by binding to and altering the structure of effector molecules. The c-di-GMP signaling network regulates many bacterial phenotypes, including flagellum- (44, 45) and pilus-mediated motility (46), biofilm formation (47), biosynthesis of quorum-sensing signal molecules (48), asymmetric cell morphology (49), virulence factor secretion, host suppression, and defense mechanisms (50). The presence of c-di-GMP typically represses motility and activates biofilm formation. While in a sessile state, c-di-GMP–modulating enzymes (CMEs) may increase c-di-GMP levels that in turn increase the exopolysaccharide synthesis (51) and biofilm production (52). Conversely, bacteria may decrease c-di-GMP concentrations to transition to a motile state by activating flagellum- or pilus-mediated motility systems (47). Diguanylate cyclases and c-di-GMP–specific phosphodiesterases are the CMEs that control the switch between the two states.

Diguanylate Cyclases Produce C-di-GMP

Diguanylate cyclases (DGCs) convert two GTPs to a single c-di-GMP molecule. The active site of DGCs contains the conserved amino acid sequence motif GG(D/E)EF. DGC domains can increase the concentration of c-di-GMP inside the cell upon activation by N-terminal sensory or regulatory modules like PAS domains (53). As the c-di-GMP concentration increases, c-di-GMP acts in a negative feedback loop by noncompetitively binding and inhibiting DGC domain activity at an allosteric inhibitory I-site (53). In this way, external signals can activate the production of intracellular c-di-GMP to a desired concentration.

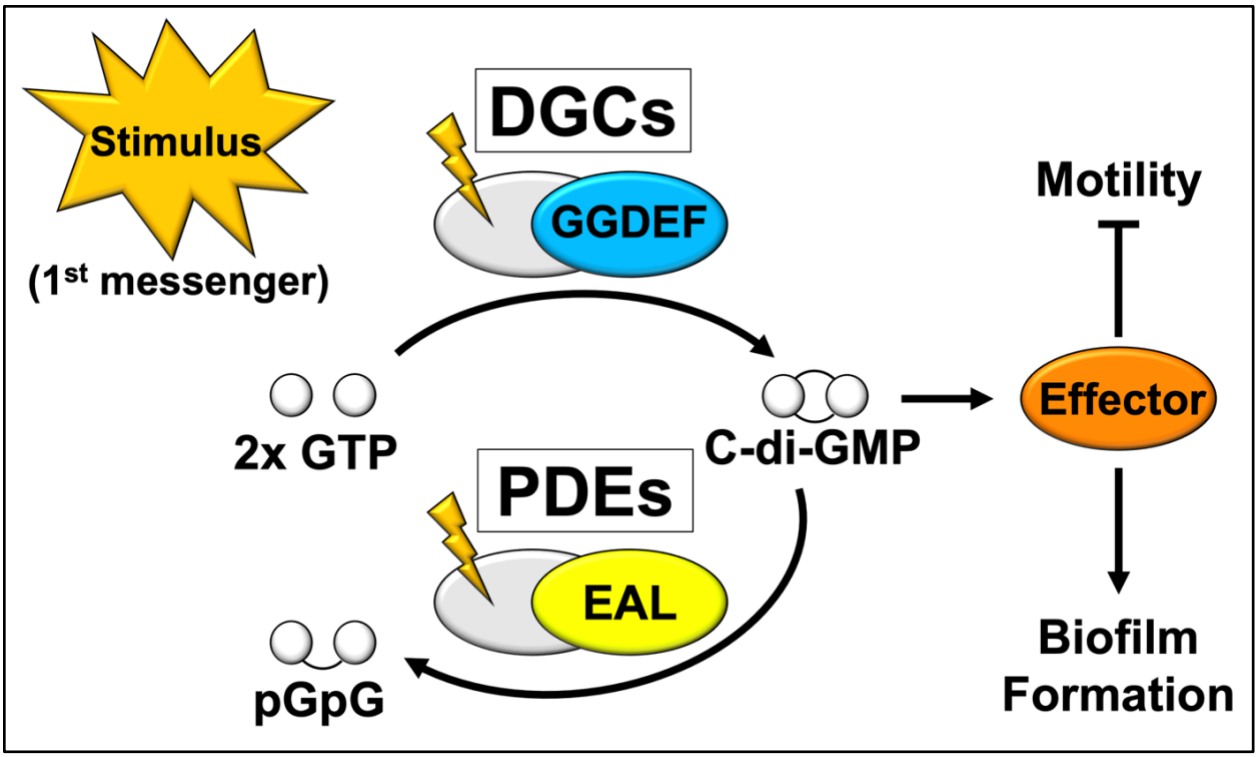

FIG 1. Simplified c-di-GMP signaling pathway

Diguanylate cyclases (DGCs) convert 2 GTP molecules to c-di-GMP, while c-di-GMP–specific phosphodiesterases (PDEs) degrade c-di-GMP to linear diguanylate (pGpG). Both DGCs and PDEs commonly encode N-terminal sensory domains that regulate enzymatic activity. C-di-GMP then binds to a variety of downstream effectors that regulate phenotypic outputs, including motility and biofilm formation.

Phosphodiesterases Degrade Endogenous C-di-GMP

Since DGCs are responsible for generating c-di-GMP, a mechanism to counteract the generation of the second messenger must be in place. C-di-GMP–specific phosphodiesterases (PDEs), encoding an EAL domain, enzymatically hydrolyze c-di-GMP to a linear diguanylate, pGpG (FIG 1) (54). Like DGCs, PDEs are often regulated through the activation of N-terminal sensory domains. In conjunction with five

other residues, the glutamate (denoted as ‘E’) in the RocR EAL domain of *P. aeruginosa* PAO1 utilizes base-catalyzed deprotonation of Mg^{2+}-coordinated water to hydrolyze intracellular c-di-GMP, implying this glutamate is obligatory for the enzyme’s catalytic activity (55-58).

In some instances, proteins contain both DGC and PDE domains in tandem—further denoted as dual domain CMEs (DCEs). Certain examples of DCEs indicate that both enzymatic domains are active and vary their activity depending on signaling through N-terminal sensory domains (59). In other cases, one domain is found in a catalytically inactive form that may play a further regulatory role upon the active domain (60, 61). One regulatory mechanism used by some of these catalytically inactive domains is through the binding of c-di-GMP itself, converting them into c-di-GMP–binding effector proteins (62, 63).

Effector Molecules Bind C-di-GMP to Regulate Phenotypes

There are varieties of c-di-GMP–binding effectors (CBEs) that include transcriptional regulators, enzymes, structural proteins, and RNA riboswitches. The most well-known c-di-GMP–binding effector domain, PilZ, appears in several different proteins. The eponymous example stems from the 1996 discovery of the *P. aeruginosa pilZ* gene that was required for type IV fimbrial biogenesis (64). The most necessary motif required for c-di-GMP–PilZ binding is the highly conserved RxxxR switch region in the N-terminus portion of the PilZ domain (65), albeit not all PilZ domain-containing downstream effectors in *P. aeruginosa* bind to c-di-GMP (66). A later study continued to investigate derivatives of c-di-GMP–binding sites in the PilZ domain-containing c-di-GMP–induced flagellar brake protein, YcgR (67). This protein has distinct roles in c-di-

GMP–dependent motility. PilZ functions with a regulatory role in twitching motility (68-70), whereas YcgR regulates swimming and swarming motility as a flagellar brake (71). More Enterobacteriaceae pathogens have been found to contain YcgR, PilZ, and PilZ domain-containing proteins in *E. coli* and *Salmonella* (71), showing that this mechanism of motility regulation is seemingly conserved among several bacterial genera.

Potential C-di-GMP Regulation of AB5075 Persistence Factors

Though c-di-GMP regulatory mechanisms haven't been studied heavily in *A. baumannii*, researchers can utilize reverse genetics and modern bioinformatics programs to pursue *A. baumannii* CMEs. Since the ESKAPE pathogens use the c-di-GMP signaling network, research in the secondary messenger signaling network can be used to discover novel antimicrobial targets. *Acinetobacter* is a concerning ESKAPE pathogen as a result of no candidate compounds in late-stage development to treat these infections (72). Due to everything outlined in this introduction, I hypothesized that c-di-GMP is a factor in the persistence of *A. baumannii*. By better understanding these phenotypes and their regulation by c-di-GMP, this information can be used for the design of strategies to combat *A. baumannii*. I outlined different physiological responses that could help *Acinetobacter* persist in a hospital and test how genes that encode CMEs and CBEs regulate *Acinetobacter*'s ability to perform these responses. This work was a comprehensive screen of annotated *A. baumannii* AB5075 CMEs and CBEs, paving the way for many future projects in the *A. baumannii* c-di-GMP field.

CHAPTER 2. RESULTS

Identification of Eleven Putative CMEs and a CBE in *A. baumannii*

My committee chair, Dr. Erik Petersen, performed a preliminary protein BLAST search for CMEs in *A. baumannii* strain AB5075 using the DGC domain from *Caulobacter crescentus* PleD protein, the PDE domain from the *Pseudomonas aeruginosa* PA2133 protein, and the *Salmonella enterica* serovar Typhimurium YcgR protein (45, 73, 74). This protein BLAST evinced a putative collection of 7 DGCs, 1 PDE, 3 DCEs, and 1 CBE putative genes (FIG 2). These genes were entered into the SMART and the CDD programs to check for domain integrity (75, 76). Two additional genes, *pde2* and *cbe2*, were also found in a second strain, *A. baumannii* 17978 (Appendix E5). A transposon mutant for *cbe2* was not available in AB5075, and we found that *pde2* is likely a pseudogene in AB5075 due to a nucleotide deletion within this gene; the reading frame shifts, leading to an early stop codon, and resulting in partial *pde2* coding. Future work will seek to generate these mutants in AB5075 and determine their functions.

To simplify the nomenclature, I altered the naming conventions of each of these genes (FIG 2). I decided that naming "*dgc1*" as "*dgcA*" could be misinterpreted as the orthologues of *dgcA* genes (77). Hence, I ordered them from *dgc1* to *dgc7* as temporary names in sequential order of the AB5075 genome. I applied the same conventions to PDEs, DCEs, and CBEs. If desired, I provided the official gene names of all genes in this study with their corresponding temporary gene names (Appendix D).

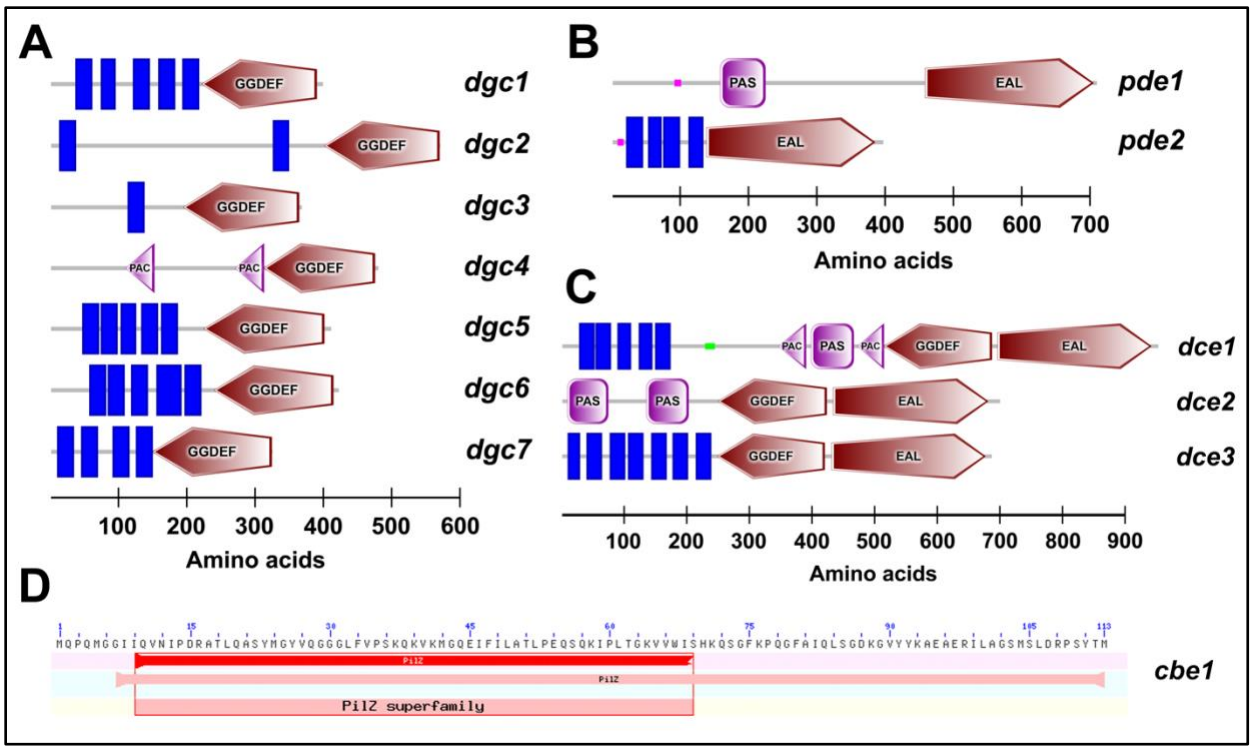

FIG 2. *A. baumannii* AB5075 encodes several putative CMEs and a CBE

A BLAST search of the genome for *A. baumannii* AB5075 identified several c-di-GMP–associated genes. SMART revealed many putative (A) diguanylate cyclases, (B) c-di-GMP–specific phosphodiesterases, and (C) dual domain-containing c-di-GMP–modulating enzymes. (D) Using the CDD, a single putative c-di-GMP–binding effector is visualized in *A. baumannii* AB5075. Gene "*cbe1*" contains a PilZ domain on the N-terminus where c-di-GMP could potentially bind to this domain. Blue rectangles show transmembrane regions; GGDEF motifs represent putative DGC domains; EAL motifs represent putative diguanylate PDE domains; and PAS/PAC motifs represent putative sensory regions.

Two CMEs and a CBE Regulate Twitching Motility in AB5075

Pilus-mediated twitching motility may play a role in *A. baumannii*'s ability to adhere and move around on abiotic surfaces either inside or outside the host. A transposon library of *A. baumannii* exists with insertions in each of the non-essential genes of the organism (78). Transposon mutants in each of the 11 putative CMEs (7 DGCs, 1 PDE, and 3 DCEs) and a single PilZ domain-containing putative CBE protein were acquired and tested for their ability to exhibit type IV pilus-mediated motility. As controls, four additional mutants were also tested: *pgaA*, *algC*, *csuA*, and *pilA*. The product of *pgaA* binds to the biofilm adhesin polysaccharide, poly-β-1,6-*N*-acetyl-D-glucosamine, *algC* codes for phosphomannomutase used for the attachment step of forming a biofilm, and *csuA* codes a primary unit for the surface adhesion pilus, so I do not expect decreased motility when disrupting these genes due to their roles in biofilm formation rather than motility. The only mutant that should result in decreased motility is the *pilA* mutant because it is the major subunit for pilus-mediated motility. Although Luria broth (LB) agar plates were made fresh before each experiment, I tried accounting for experimental variability by comparing the results of the individual mutants to the distance traveled by wild-type AB5075 for each experiment (FIG 3).

As expected, interruption of the *pilA* type IV pilin gene blocks all twitching motility, while none of the *pgaA*, *algC*, or *csuA* mutants exhibit altered motility. Two CME mutants, *pde1* and *dce1*, exhibited reduced motility; loss of *pde1* rendered the strain non-motile, similar to deletion of the *pilA* gene, while *dce1* appears to be partially responsible for full motility in AB5075. Secondly, loss of *cbe1* stunted motility entirely, showing that it is a key player in pilus-mediated motility.

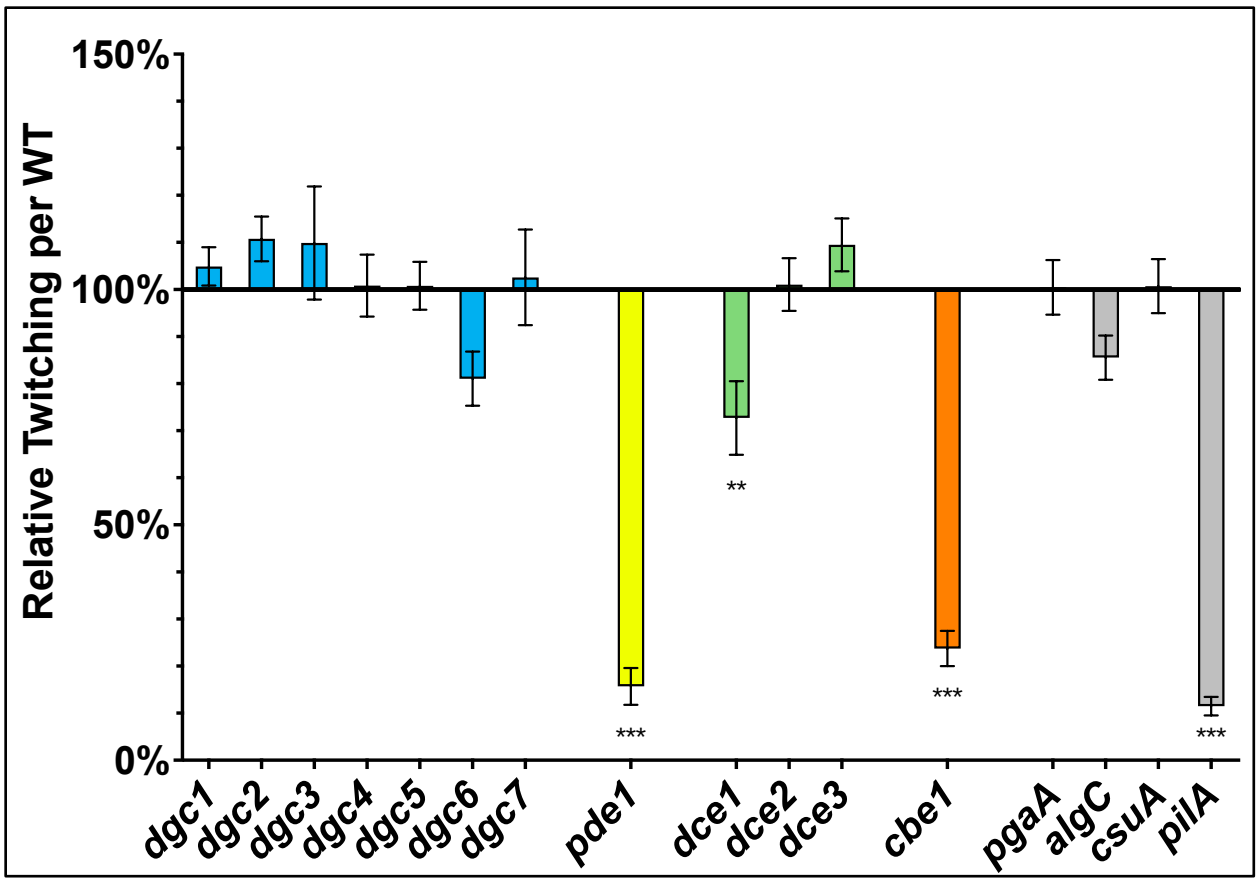

FIG 3. Transposon mutations in *pde1*, *dce1*, and *cbe1* alter twitching in AB5075

Overnight cultures of transposon mutants were inoculated into the center of a 0.4 % LB agar plate, stabbed through the agar to the plastic Petri dish bottom, and incubated at 37 °C inverted overnight. The next day, perpendicular diameters of the region of motility were measured and determined significance using ANOVA with Dunnett's post hoc test (against a control: wild-type AB5075). Shown is the relative change in distance traveled of each strain (± SEM) versus wild type (at 100 %). n=6. ** = $p<0.01$, *** = $p<0.001$

I proceeded by generating complement strains with the pMMB-RIF vector expressing the gene of interest (FIG 4). The complement plasmids were induced by including 1 mM isopropyl β-D-1-thiogalactopyranoside (IPTG) into the agar motility plates. (FIG 4). The restoration of the genes should return twitching motility to wild-type levels. I also included a negative gene-absent pMMB-RIF empty vector (pEV) control into each mutant and wild type which looks identical to the image of the expression vector (FIG 4); with this, I can ensure any increase in motility is due to the reintroduction of the gene and not a confounding variable. Additionally, I included two positive controls in wild type (WT) with a DGC and PDE.

The complements restored twitching abilities to wild-type levels in all three strains (FIG 5). It appears that *pde1* and *cbe1* are required for twitching motility under these conditions, while *dce1* plays a partial role in motility. Since both enzymatic domains are annotated in *dce1*, I confirmed whether varying *dce1* expression levels affects motility; to modify the expression level of pMMB-RIF, I treated LB agar plates with varying concentrations of IPTG. I inoculated these LB agar plates with the WT+pEV, *dce1*+pEV mutant, or *dce1*+p*dce1* complement (FIG 6). I found that *dce1* activity remains constant to wild type regardless of expression levels. In this section, I showed that CMEs regulate twitching motility; this data suggests that *A. baumannii* AB5075 uses c-di-GMP and a CBE to regulate type IV pilus-mediated motility—a factor that may help AB5075 travel and persist on hospital surfaces.

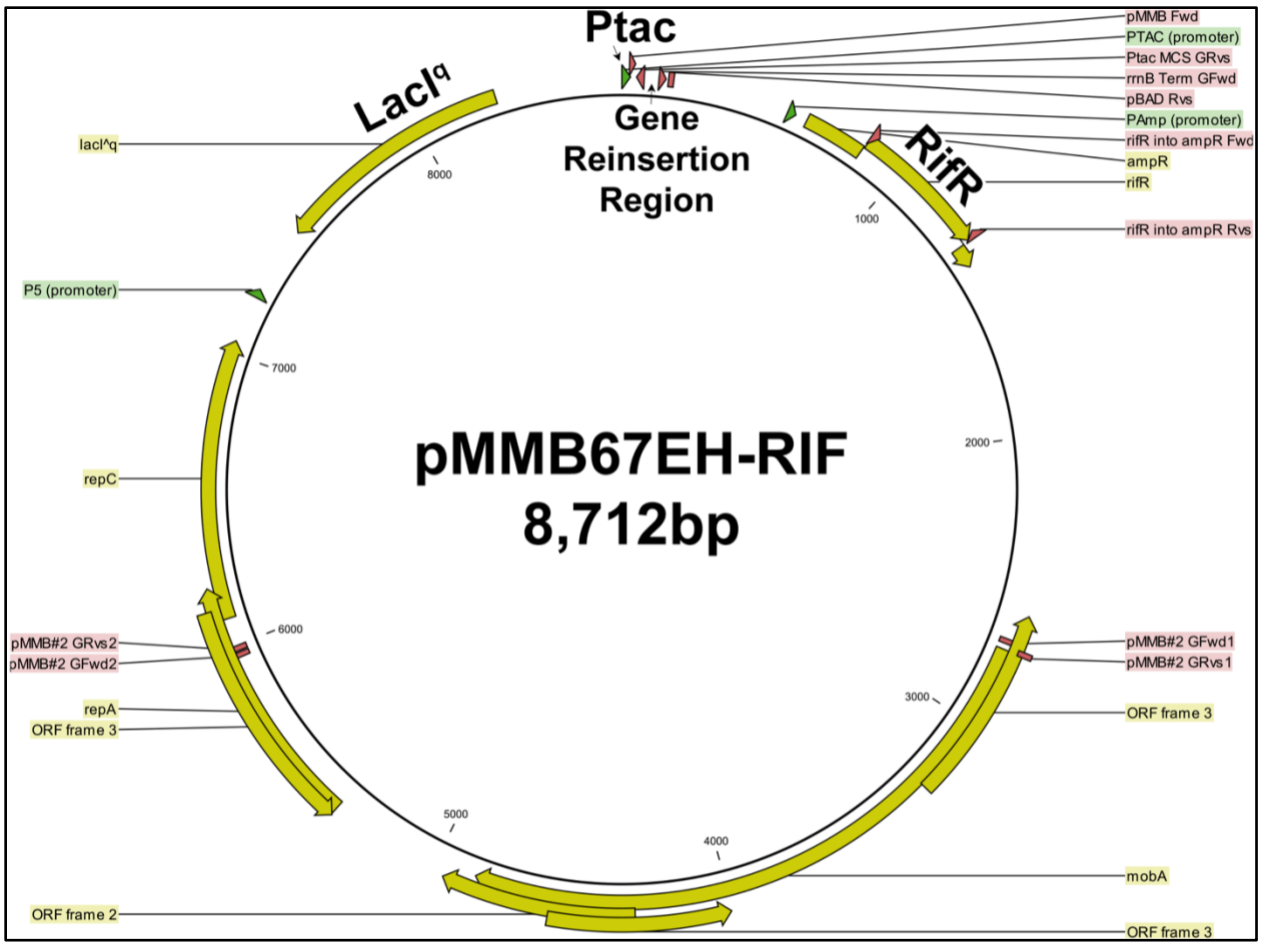

FIG 4. The pMMB67EH-RIF expression vector map

The above expression vector, pMMB67EH-RIF, was used as the complement vector for this study to express a gene insertion using Ptac (the *tac* promoter)—a portmanteau for the *trp* and *lac* operons. $LacI^q$ represses the *lac* operator by binding to the –10 coding region to prevent transcription of downstream genes. IPTG, an allolactose isomer, mimics allolactose to induce pMMB67EH-RIF by derepressing the *lac* operator and thus permitting transcription (79). Since *A. baumannii* is already resistant to ampicillin, I inserted rifampicin resistance (RifR) in lieu of the ampicillin cassette for plasmid confirmation and retention. The genes of interest were situated in the “Gene Reinsertion Region.” Please refer to this reference if additional information is desired (80).

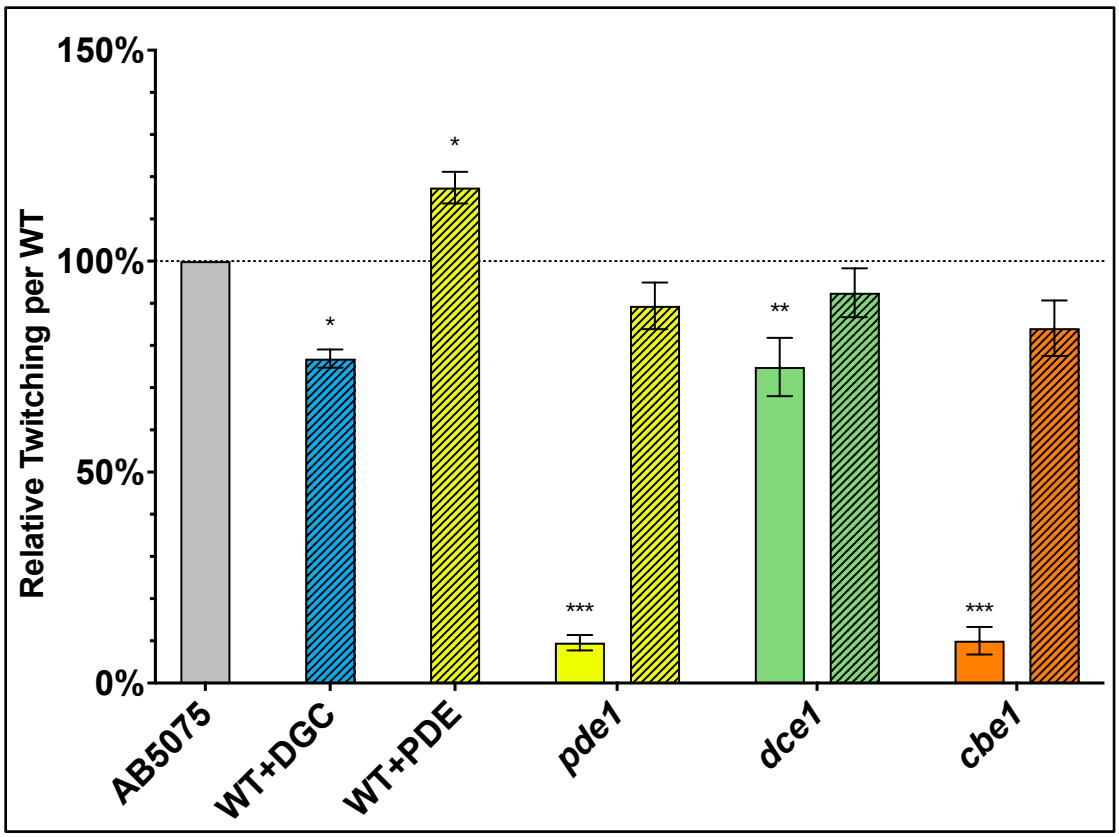

FIG 5. AB5075 mutant complements replenish twitching motility from *pde1*, *dce1*, and *cbe1* gene reinsertions

Strains containing pEV are denoted as clear (▭), whereas complemented strains are denoted by diagonal lines (▨). Overnight cultures of the above complemented mutants were inoculated into the center of LB plates with 0.4 % agar, 1 mM IPTG, and 50 µg/mL rifampicin. The culture was then stabbed through the center to the plastic bottom of the Petri dishes and incubated overnight at 37 °C. Perpendicular diameters of the motility regions were measured and determined significance using ANOVA with Dunnett's post hoc test (against a control: AB5075 WT+pEV). Shown is the relative distance traveled of each strain (± SEM) versus the WT+pEV (at 100 %). n=6. ** = $p<0.01$, *** = $p<0.001$

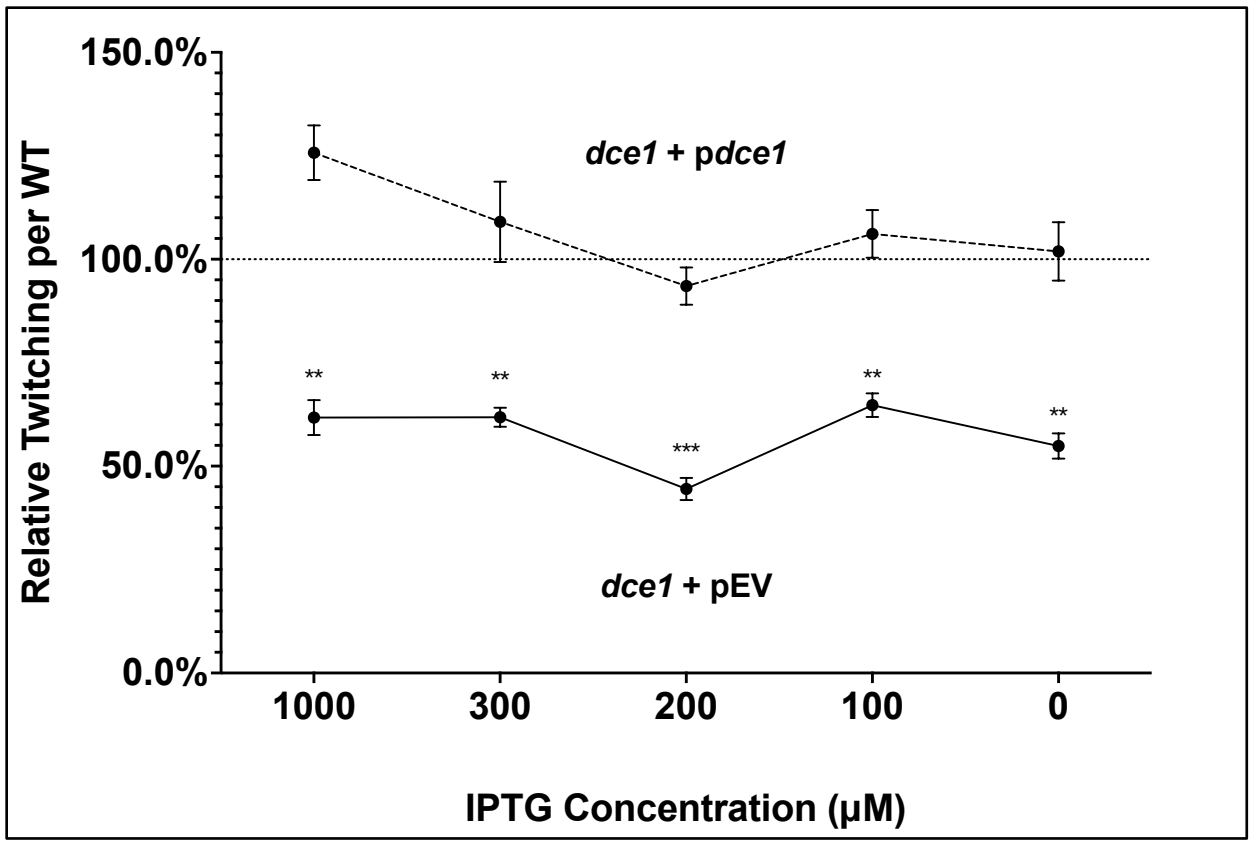

FIG 6. Several expression levels complement the *dce1* mutant of AB5075

The dotted line indicates the *dce1*+p*dce1* while the solid line represents the *dce1*+pEV. Overnight cultures of WT+pEV, *dce1*+pEV, and *dce1*+p*dce1* were inoculated into the center of LB plates with 0.4 % agar, 1 mM IPTG, and 50 μg/mL rifampicin. The inoculated culture was then stabbed through the center to the plastic bottom of the Petri dishes and incubated overnight at 37 °C. Perpendicular diameters of the motility regions were measured and determined significance using two-way ANOVA with Greenhouse-Geisser correction and Dunnett's post hoc test (against a control: AB5075 WT+pEV). Shown is the relative distance traveled of either strain (± SEM) versus the WT+pEV (at 100 %). n=4. ** = $p<0.01$, *** = $p<0.001$

Multiple CMEs Regulate Biofilm Formation in AB5075

Biofilms are a common mechanism used by a wide range of bacteria to survive in environmental or infectious settings where they may need to withstand incoming stress. The AB5075 transposon mutants were screened in LB for their ability to produce biofilm within a polystyrene 96-well plate. Detection of biofilms was done using a 0.1 % crystal violet and Milli-Q® ultrapure water staining solution that was resuspended in 95 % ethanol to measure the optical density at 595 nm. Several DGC disruptions, the *pde1* disruption, and disruption of *dce2* and *dce3* resulted in decreased biofilm production by about 50 % of the WT (FIG 7). Upon further examination, the *pde1* mutant exhibits reduced growth when under the non-shaking conditions used for biofilm formation assays. Examination of this growth phenotype will be required to determine whether any true change in biofilm formation is occurring in the *pde1* mutant. Complementation plasmids for the significantly disrupted mutants were generated, transferred to the mutant strains alongside an empty vector control, and tested under complementation-inducing conditions. Positive controls for both a DGC and a PDE were included in the complement tests to confirm whether the results are attributable to c-di-GMP. The DGC and PDE positive controls increased and decreased biofilm levels, respectively, suggesting c-di-GMP can play a role in *A. baumannii* biofilm formation (FIG 8). Further, the biofilm-producing phenotype either exceeded or restored wild-type levels in all six DGC complements (FIG 8). Transfer of the complementation plasmid in the *dce3* mutant strain was unsuccessful, so additional work will need to be done to determine the role of Dce3 in biofilm formation.

When the *dce2* plasmid complement was inserted and induced, biofilm production was reduced even greater than the transposon mutant alone (FIG 8). This would suggest that complementation didn't properly work, but *dce2* may code for a DCE that may contain both DGC and PDE activities. By inducing the complementing plasmid with IPTG levels from 0 μM to 8,000 μM, I showed that low levels of *dce2* induction successfully complemented the transposon mutant (FIG 9). Nonetheless, this data suggests that *A. baumannii* AB5075 regulates biofilm formation by c-di-GMP using several DGCs and a DCE with seemingly active DGC and PDE domains. Biofilm formation is a widely known phenotype that helps bacteria persist, especially in hospital settings. This study shows that genes coding for c-di-GMP modulators affect biofilm formation significantly in *A. baumannii* AB5075.

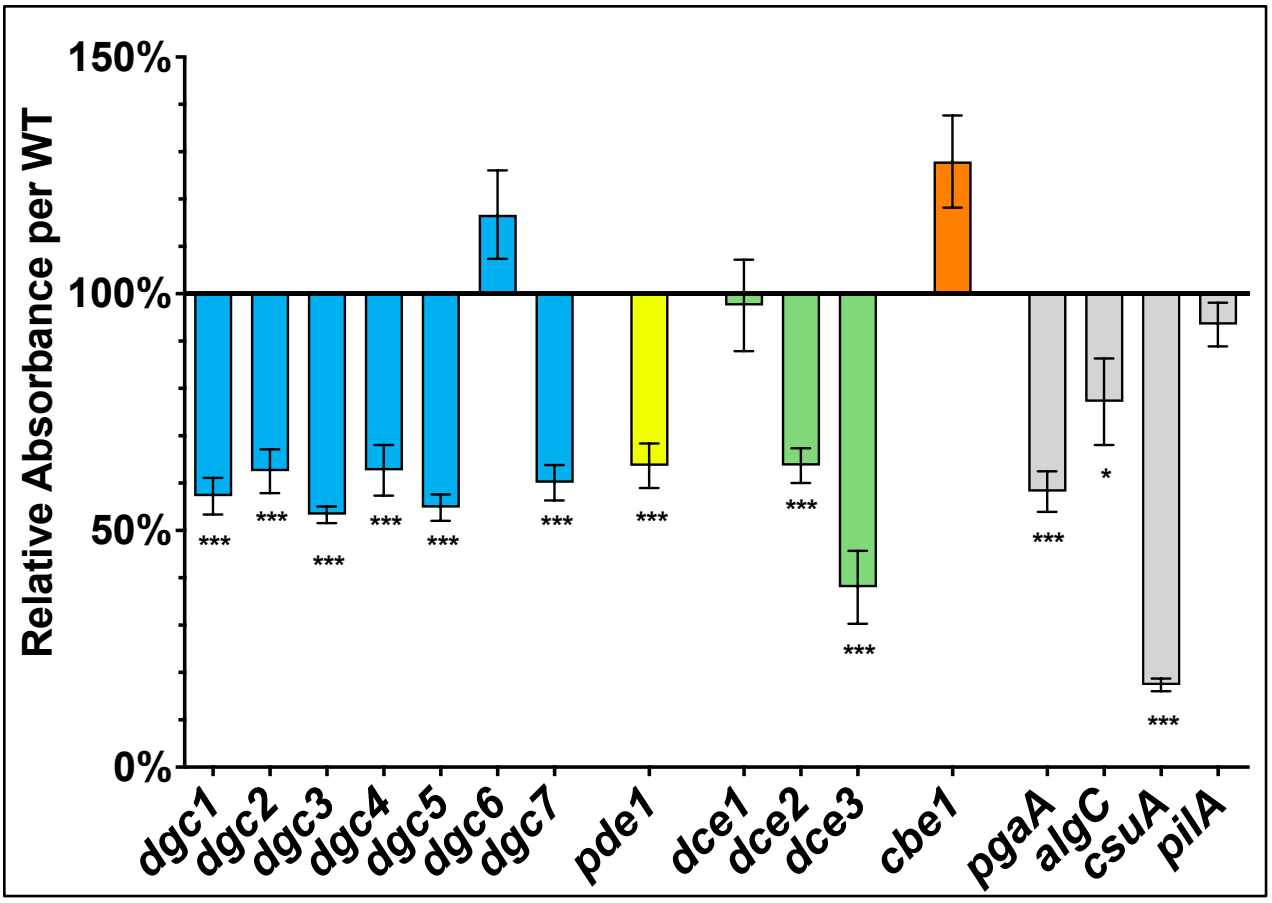

FIG 7. Transposon mutations of many CMEs alter biofilm levels in AB5075

Overnight cultures of transposon mutants were diluted to 0.05 OD_{600} and grown in LB overnight at 37 °C in 96-well plates. The 96-well plates were then washed in distilled water, stained with 0.1 % crystal violet, and quantified by dissolving the adhered crystal violet dye with 95 % ethanol. The OD_{595} of the released crystal violet was measured and compared to AB5075 wild type using ANOVA with Dunnett's post hoc test. Shown is the relative change of the measured OD_{595} of each strain (± SEM) versus the wild type (at 100 %). n=6. *** = $p<0.001$

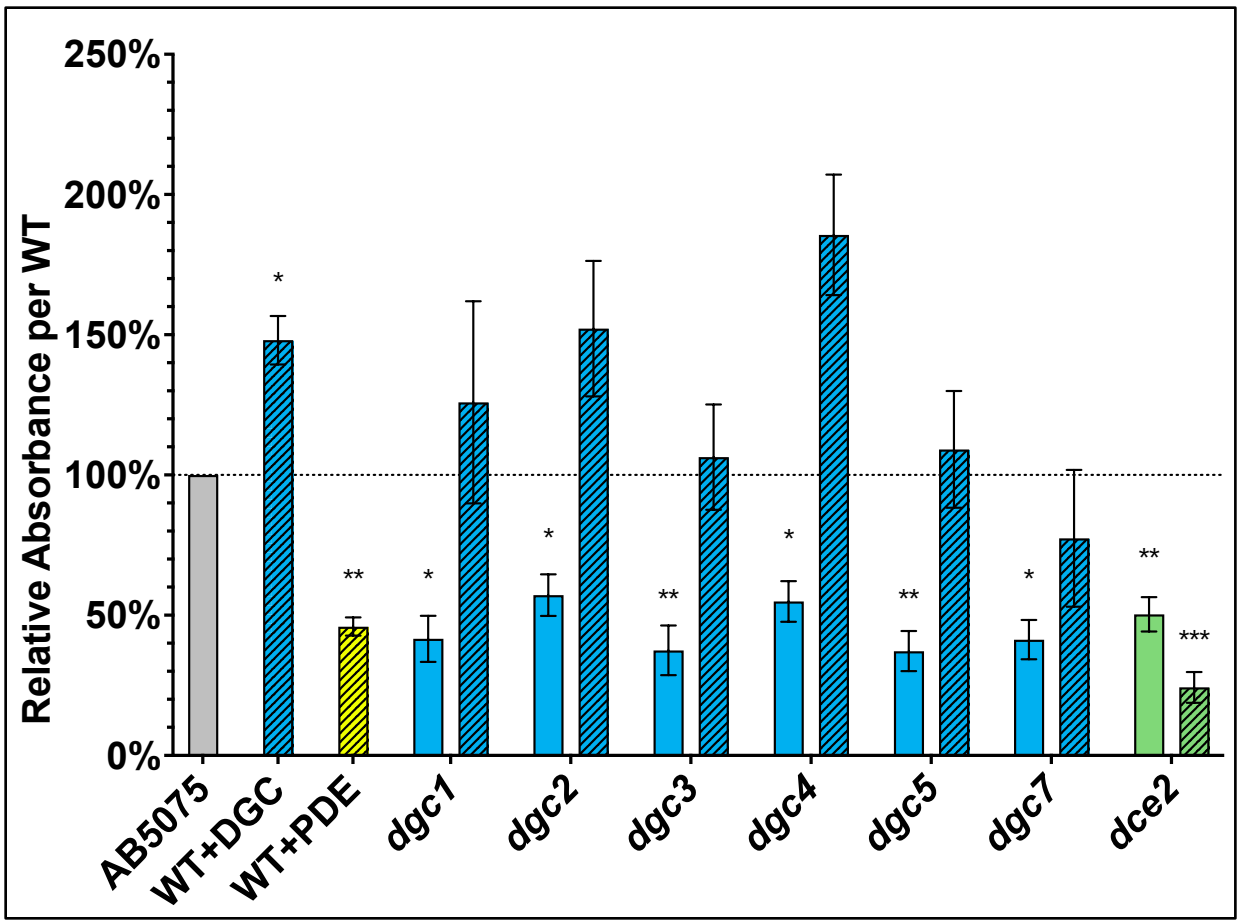

FIG 8. Complemented *dgc* mutants restore WT biofilm levels in AB5075

Strains containing pEV are denoted as clear (▭), whereas complemented strains are denoted by diagonal lines (▨). Overnight cultures of complemented AB5075 mutants were diluted to 0.05 OD_{600} and grown overnight at 37 °C in 96-well plates with LB, 1 mM IPTG, and 50 µg/mL rifampicin. The 96-well plates were then washed in distilled water, stained with 0.1 % crystal violet, and quantified by dissolving the adhered crystal violet dye with 95 % ethanol. The OD_{595} of the released crystal violet was measured and compared to AB5075 WT+pEV using ANOVA with Dunnett's post hoc test. Shown is the relative OD_{595} of the mutant (± SEM) compared to WT+pEV. n=6. * = $p<0.05$, ** = $p<0.01$, *** = $p<0.001$

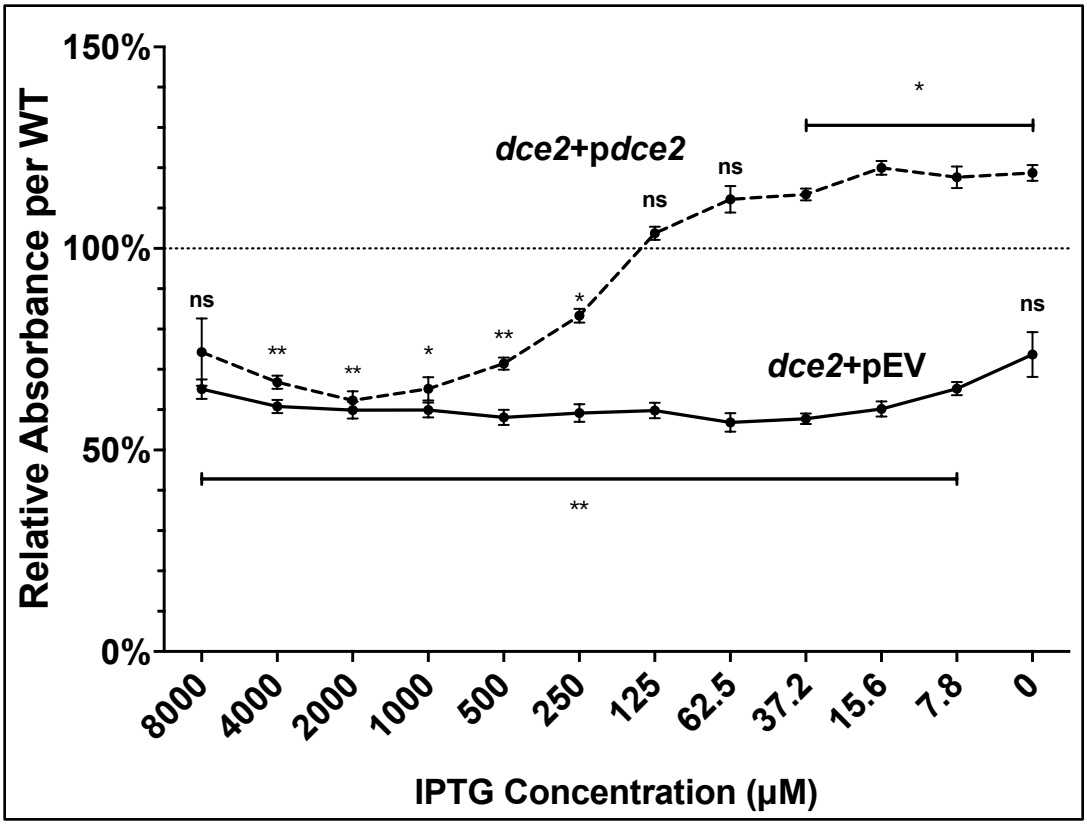

FIG 9. Different expression levels complement and reveal the *dce2* mutant contains DGC/PDE activity for biofilm production in AB5075

The solid line represents *dce2*+pEV, whereas the dashed line represents the *dce2*+p*dce2* complement. Overnight cultures of *dce2* mutants were diluted to 0.05 OD_{600} and grown overnight at 37 °C in 96-well plates with L, 50 μg/mL rifampicin, and concentrations of IPTG from 0 μM to 8,000 μM. The 96-well plates were washed in distilled water and stained with crystal violet. The OD_{595} of the released crystal violet was measured and compared to WT+pEV using two-way ANOVA with Greenhouse-Geisser and Dunnett's post hoc test. Shown is the relative change of the measured OD_{595} of both mutants (± SEM) versus the WT+pEV (at 100 %). Capped lines show that each point within the bounds is significant to the noted degree. n=3. * = $p<0.05$, ** = $p<0.01$

DGC and CBE Regulation of Desiccation Tolerance in AB5075

A. baumannii is also capable of surviving on dry surfaces for an extended period of time, providing a reservoir for infection within hospital settings. To determine whether c-di-GMP plays a role in desiccation survival, the *A. baumannii* AB5075 transposon mutants were screened for their ability to survive desiccation environmental stress by CFU counts. In AB5075, the *dgc6* and *cbe1* mutants resulted in a significant decrease in CFU/mL of 342- and 60-fold, respectively (FIG 10). Likewise, a second *A. baumannii* strain, 17978, showed a decrease in desiccation tolerance in *dgc6* and *cbe1* of 88- and 9-fold, respectively (Appendix E4). It seems that ridding the cell of specific DGCs may harm the ability to survive after experiencing water scarcity for 48 hours. Though further work still includes complement tests, *A. baumannii* appeared to have lower desiccation survival when disrupting the coding sequences of *dgc6* and *cbe1*, suggesting a role for c-di-GMP in regulating this phenotype (FIG 10 and Appendix E4).

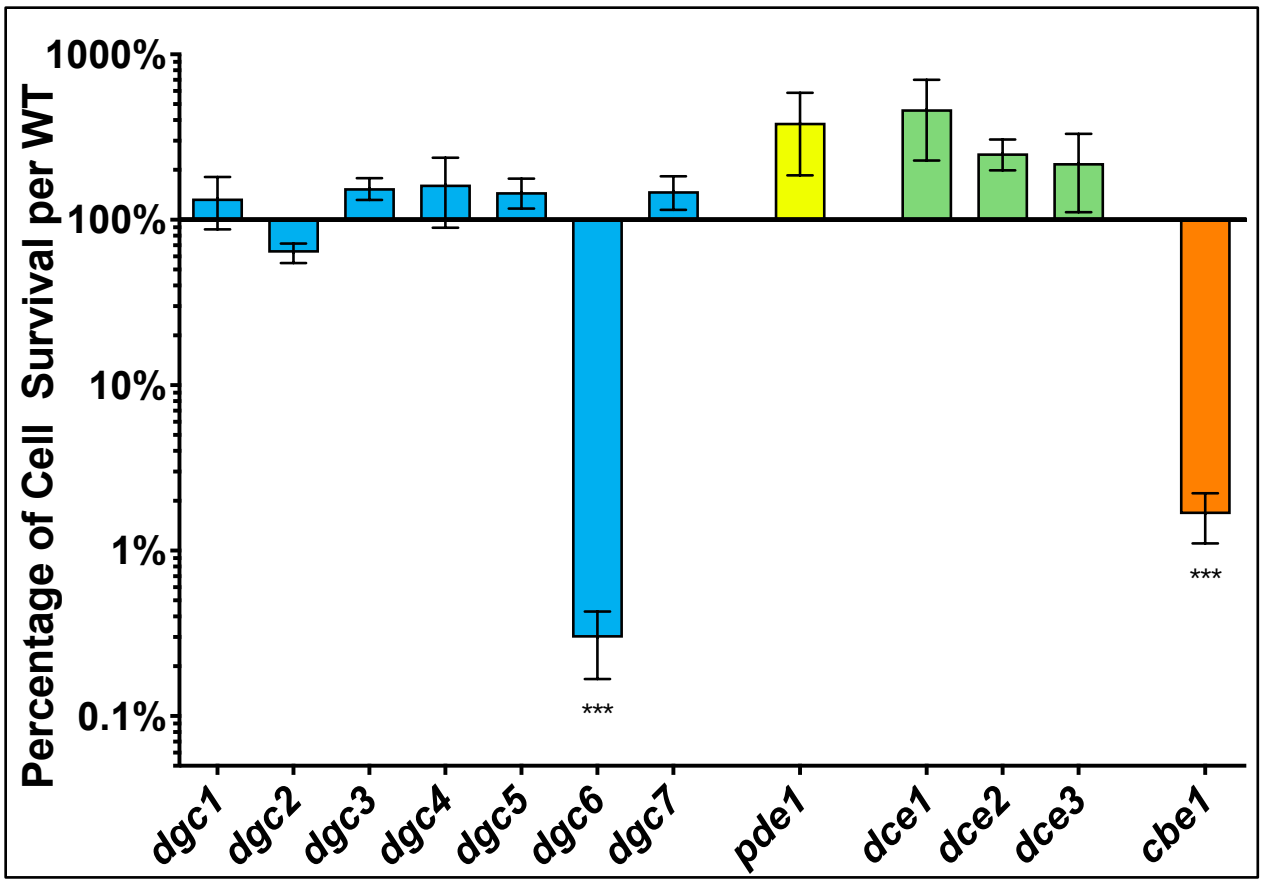

FIG 10. Transposon mutations of genes *dgc6* and *cbe1* determine survival after 48-hour exposure to a desiccating environment in AB5075

Overnight cultures of transposon mutants were washed and diluted with distilled water. One 96-well plate was dried for 48 hours, and a separate 96-well plate was used to serially dilute cultures to a countable number of colonies. After 48 hours, the same was done to the dried 96-well plate. Colony-forming units were converted to colony-forming units per mL to compare mutants to the wild-type value. ANOVA with Dunnett's post hoc test was used to compare each mutant to the wild type. Shown is the percentage of cell survival per wild type (± SEM) and is defined as the CFU/mL of mutants divided by the CFU/mL of wild-type AB5075 (at 100 %). n=5. *** = $p<0.001$

CHAPTER 3. DISCUSSION

CME Regulation of Persistence Factors in AB5075

In this thesis, I identified a putative role for c-di-GMP regulation of motility, biofilm formation, and desiccation tolerance in *Acinetobacter baumannii* AB5075. By identifying several genes that contain domains known to regulate c-di-GMP levels, I was able to test my hypothesis using transposon-disrupted mutants of AB5075. (FIG 3, FIG 7, and FIG 10). Before this study, there was no evidence that AB5075 utilized c-di-GMP to persist in dangerous conditions. Only recently, *A. baumannii* 17978 CMEs were shown to be active when overexpressed *in vitro* to regulate biofilm formation and surface motility, an alternative motility type to twitching (47). I showed that these CME and CBE genes are beneficial to AB5075 because disrupting the coding sequences causes a decrease in twitching motility (FIG 3), the production of biofilm (FIG 7), and its survival under desiccating conditions (FIG 10). Since CMEs alter the levels of c-di-GMP, the influence that these genes have on the cell's physiology suggests that c-di-GMP is used for these phenotypes that may aid the persistence of *A. baumannii* on hospital surfaces.

Previous studies have already shown several factors including quorum sensing, light, iron availability, and inactivation of type IV pili, among others that influence *A. baumannii* motility (24-27, 81-86) and sessility (36, 37, 40, 41, 87), as previously mentioned. In this study, I showed that there is another regulator in *A. baumannii* between these two states: c-di-GMP. Widely found in many bacterial organisms, c-di-GMP is known to halt motility in *P. aeruginosa* and *E. coli*, among other species (68-71).

With movement ceased, bacteria transition to a defensive state by encasing themselves within a biofilm, and particularly in this study, AB5075 does, too.

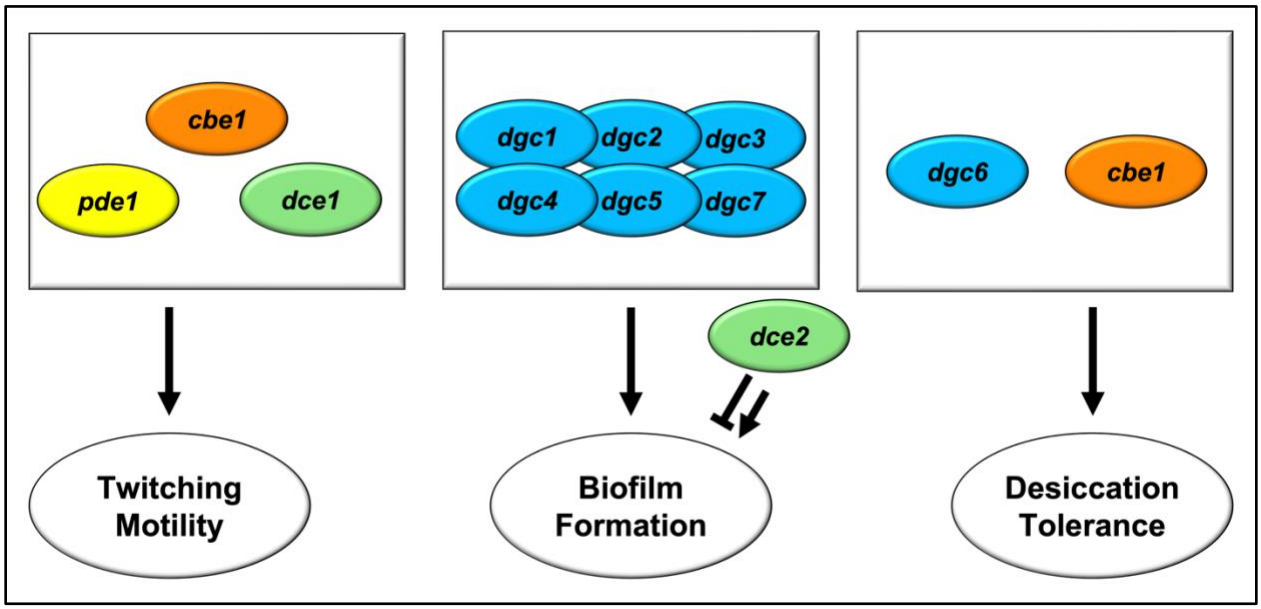

FIG 11. AB5075 CME/CBE regulation of physiological responses

The results of the AB5075 strains are shown. Blue represents DGCs; yellow, PDEs; green, DCEs; and orange, CBEs. The arrows point to activation of a physiological responses while a capped line points to suppression of a physiological response.

By heterologously expressing a known DGC and PDE in AB5075, I showed that there is an effect these CMEs have in this strain. When inducing a DGC, biofilm production levels increased significantly; conversely, induction of a PDE in AB5075 decreased biofilm production levels (FIG 8). These results give a foundational exhibition of DGC and PDE activity within AB5075 and support the hypothesis that c-di-GMP regulates *A. baumannii* biofilm formation. With that information, I then tested the disruption of CME genes within the *A. baumannii* genome and whether these CMEs

were required for biofilm formation. Several DGCs were required for wild-type levels of biofilm formation, and many of the *A. baumannii* genes acted similarly to the *P. aeruginosa* DGC and PDE when overexpressed in *A. baumannii*. Not only are non-CME genes in *A. baumannii* attributable to the production of biofilm biomolecules (28, 29, 35-38, 41), but c-di-GMP should be another recognized regulator between biofilm formation and motility in the AB5075 isolate.

Motility

While individual stains of *A. baumannii* can exhibit different types of motility, I wanted to see if c-di-GMP would affect twitching motility of AB5075. As surface-associated motility in *A. baumannii* strain 17978 has previously been shown as regulated by c-di-GMP (47), I also compared gene deletions in the CMEs within that strain (Appendix E1); the *pde1* gene was a major regulator of twitching motility in *A. baumannii* AB5075 (FIG 5) but did not show a profound effect on surface motility of the second *A. baumannii* strain, 17978. Conversely, the *pde2* gene was a major regulator of surface motility in 17978 but is a pseudogene in AB5075. It is possible that as the ancestors of AB5075 were selectively pressured to twitch rather than translocate on surfaces; *pde2* was no longer active in AB5075, forcing it to rely solely on twitching. 17978 still contains the mechanism for surface motility and the regulation of this motility with the *pde2* CME-encoding gene. Deletion of either PDE could support the idea that high c-di-GMP, generated by the loss of this PDE activity, reduces motility in AB5075.

One of three DCEs, *dce1*, exhibited significantly decreased motility in AB5075 (FIG 5); while the remaining two DCEs, *dce2* and *dce3*, were responsible for a

significantly deleterious biofilm formation in AB5075 (FIG 8). Thus, I confirmed the *dce2* dual-domain activity in biofilm formation, which appeared to have an antagonistic effect on itself (FIG 9). Because of the *dce2* activity, I wanted to see if *dce1* would experience a similar effect on twitching motility (FIG 6). I did not witness an obvious transition between putative DGC and PDE activities (FIG 6). One hypothesis would be that Dce1 only encodes a single active domain or that the protein plays a structural or regulatory role in twitching motility, but further analysis of *dce1* by inactivation of the enzymatic domains through site-directed mutagenesis or some similar method needs to be done to fully understand its role in c-di-GMP modulation of motility.

The complete absence of twitching motility in the *cbe1* mutant suggests that it is at least necessary for pilus-mediated motility in AB5075; *cbe1* shows high homology to the *P. aeruginosa pilZ* gene, so *cbe1* may simply be necessary for the stability of the pilus—not dependent on c-di-GMP levels. The gene disruption may halt pilus operation due to *cbe1* not binding to a binding partner, removing communication to the pilus subunits (88); an inability to assemble the pilus like in *P. aeruginosa* (70); or the PilZ domain being unavailable for c-di-GMP binding, reducing some manner of c-di-GMP signaling. When I tested the presence of motility in *A. baumannii* 17978, *cbe1* and *cbe2* showed a significant decrease in surface motility (Appendix E1), so future studies should test a *cbe2* AB5075 mutant to check for *cbe2* regulation of pilus-mediated motility.

Biofilm Formation

A. baumannii AB5075 showed a dual-domain CME and several DGCs that were necessary for biofilm regulation (FIG 7). A previous study overexpressed *A. baumannii* 17978 CMEs and concluded that *dgc2* and *dgc4* activated biofilm formation in 17978 (47). This suggests that c-di-GMP could play a regulatory role in *A. baumannii*; so when I expressed *dgc2* and *dgc4* genes with 1 mM IPTG, these mutants exhibited very high levels of biofilm formation (FIG 8). High biofilm levels when overexpressing these genes explain the activation of biofilm formation conclusion. Although in AB5075, the *dgc2* and *dgc4* genes are not the only ones necessary for biofilm formation. When disrupting their coding sequences, six of the seven DGCs showed drastic decreases in the levels of detectable biofilms (FIG 7). Heterologous expression of a DGC leads to a similar increase, while a heterologous PDE significantly decreased biofilm levels (FIG 8). This indicates that AB5075 may use c-di-GMP to regulate biofilm formation through several different DGCs that are activated within this rich medium.

The previous study on overexpression of 17978 genes also concluded that *dce2* and *dce3* overexpression inhibited biofilm formation (47). Conversely, transposon disruptions of both *dce2* and *dce3* decreased biofilm formation in AB5075. When I induced *dce2* at 1 mM IPTG, I saw similarly high levels of biofilm repression (FIG 8). Consequently, I varied the levels of IPTG and found that *dce2* can vary between phenotypes for biofilm regulation, suggesting that it may encode dual DGC and PDE activity (FIG 9). Currently, I have shown that only *dce2* is capable of both DGC and PDE activities, but confirmation of *dce3* is the next goal.

During the biofilm formation assay, I also observed a reduction in the growth of the *pde1* mutant under the non-shaking conditions used which resulted in lower biofilm detection. This may be due to decreased aeration when shaking is absent, which could mean that the *pde1* mutant requires higher oxygen levels. Whether this is also inhibiting the twitching motility phenotype is unknown. However, complementation of the *pde1* mutant during twitching motility assays was sufficient to restore motility, while attempted complementation in the biofilm formation assays did not restore growth (data not shown).

Desiccation Tolerance

Desiccation tolerance is a known phenotype in *A. baumannii* (15, 42, 43), and c-di-GMP has been linked to dryness survival as an indirect regulator (e.g., alginate production and EPS) in *Azotobacter vinelandii*, *Listeria monocytogenes*, and *P. aeruginosa* (89-92). Hence, I checked if *A. baumannii* regulates desiccation survival using a c-di-GMP pathway akin to these other organisms. In *A. baumannii* AB5075, the *dgc6* transposon mutant exhibited a 342-fold decrease in survival, and the *cbe1* mutant exhibited a 60-fold decrease in survival after 48-hour drying (FIG 10). Possibly, *cbe1* codes for the effector that regulates desiccation tolerance in response to c-di-GMP generated by Dgc4. Notably, both *dgc6* and *cbe1* were not significant in the biofilm formation assay, and these transposon mutants significantly decreased the survivability in desiccating conditions, showing that *dgc6* and *cbe1* were necessary during desiccation tolerance (FIG 10) and not biofilm production (FIG 7). This brings us to an interesting, yet unanswered, question: why are *dgc1-5* and *dgc7* disruptions deleterious

to biofilm production, while the *dgc6* disruption is harmful during dryness? Perhaps the *dgc6* mutant's desiccant-intolerable phenotype could be activated specifically during water-deficient periods, whereas the DGCs necessary for biofilm production are either not controlled by the presence of water or are activated during periods of excess water. Whatever the mechanism, these results indicate that survival during extreme dryness may be c-di-GMP–dependent in AB5075 and provide future avenues to investigate c-di-GMP–regulated desiccation tolerance in this strain.

Concluding Remarks

Genes *pde1* and *pde2* were responsible for twitching (FIG 5) and surface (Appendix E2) motilities, respectively. Also, the *P. aeruginosa* PDE positive control increased motility past wild-type levels (FIG 5). The *pde1* and *pde2* genes responsible for motility fit the original model of c-di-GMP regulation of motility (FIG 1). Perhaps these PDEs are constantly active to rid the cell of c-di-GMP keeping the cell in a motile state since coding excessive Pde1 does not enhance motility (FIG 5).

DCEs showed profound effects on both biofilm formation and twitching motility. Gene *dce1* was required for twitching motility (FIG 6), while *dce2* and *dce3* appeared to be required for biofilm formation (FIG 8). Expression of *dce2* at varying levels with IPTG produced a biofilm formation phenotype exhibiting enzymatic activities consistent with both DGC and PDE domains (FIG 9).

6 DGC genes were shown to regulate biofilm formation in AB5075 (FIG 8), while the outstanding DGC was responsible for desiccation tolerance (FIG 10). Perhaps the DGC that influences desiccation survival is only active during times of drought. Since

DGCs produce c-di-GMP to modulate levels of this molecule, c-di-GMP could likely be a regulator of desiccation tolerance. Measuring c-di-GMP levels in each of these assays would provide more evidence for this conclusion.

Overall, these data provide baseline evidence of c-di-GMP's role in regulating the surface persistence of a multidrug-resistant *A. baumannii*. Further inquiry about these data is necessary to identify the complete mechanism c-di-GMP has on this emergent strain including measurement of c-di-GMP and inactivation of active sites for DGCs or PDEs. Though merely a single step, my study provides the groundwork for the exploration into the involvement of the c-di-GMP pathway on these phenotypes in AB5075 and the potential future development of novel disinfectants and antimicrobials against this nascent pathogenic threat.

CHAPTER 4. MATERIALS AND METHODS

Bacterial Strains and Growth Conditions

Bacterial strains and plasmids are shown in Appendices A and B, respectively. Strains were typically grown with 2 to 3 mL of LB overnight 20–24 hours at 37 °C with shaking at 250 rpm. The LB contained 10.0 g/L Fisher BioReagents™ tryptone, 5.0 g/L Fisher BioReagents™ yeast extract, and 10.0 g/L Fisher BioReagents™ NaCl. Typical LB agar plates were prepared with all the LB components plus 15 g/L Fisher BioReagents™ bacteriological agar. When necessary, rifampicin was added to the medium to a concentration of 50 µg/mL, tetracycline to a concentration of 10 µg/mL, gentamicin to a concentration of 30 µg/mL, and kanamycin to a concentration of 50 µg/mL. Expression from complement vectors was accomplished by the addition of 1 mM IPTG unless otherwise indicated. Bacterial strains were stored in their original growth medium containing their corresponding antibiotic, glycerol added to 20 %, and kept indefinitely at –80 °C.

Generation of Mutant Strains

AB5075 Transposon Mutants

The original AB5075 Tn26 mutants were generated by Gallagher et al. (78) using transposome electroporation and selected for transposon insertion of tetracycline resistance on an LB agar plate. Years after their original isolations, some cells lost tetracycline resistance, so I reisolated the –80 °C stock cultures on 10 µg/mL tetracycline LB plates and picked isolated colonies. I confirmed whether they retained

the transposon by standard PCR using one primer within the gene of interest and a second within the transposon (Appendix C). 50 µL DNase-free H_2O was placed into a PCR tube, colonies from plates were suspended in the water, and they were boiled at 98 °C for 10 minutes to lyse the cells. The boiled product was centrifuged for 5 minutes at 5500 rpm. The supernatant was used as the DNA template for future PCRs. Confirmation PCRs were accomplished with Go*Taq* 2X Master Mix, which was diluted in half by adding to a PCR mix including 0.2 µM Forward Primer, 0.2 µM Reverse Primer, 1 µL template DNA, and DNase-free H_2O to final volume. For *Taq* 2X Master Mix, the extension time was set to 72 °C for 1 min/kb. PCR products were run out in a 1.0 % agarose gel by electrophoresis with the 1 Kb Plus DNA Ladder as a base pair length reference and checked for appropriate size based on the known insertion site.

AB5075 Complement Mutants

Complement vectors for *A. baumannii* AB5075 mutants were generated by Gibson assembly (93) of the gene of interest into the IPTG-inducible pMMB-RIF expression vector (FIG 4). Phusion™ Plus DNA Polymerase was added at 1 % to a PCR mix including 1X Phusion™ Plus Buffer, 0.5 µM Forward Primer, 0.5 µM Reverse Primer, 200 µM each dNTP, 2 % template DNA, and water to final volume. 40 cycles of the following were performed: the denaturation step was set to 98 °C for 30 s, the annealing step was set to 60 °C for 30 s, and the extension step was set to 72 °C for 30 s/kb. To generate the complement vectors using Gibson assembly, gene and vector fragments were made by PCR using primers containing 30 base pair overlaps. The fragments were included in a Gibson assembly master mix and incubated in a thermal cycler for 60 minutes at 50 °C. During incubation, all DNA fragments will produce a

complete vector construct by binding at pre-defined homologous overlaps designed within the sequences. Vectors were chemically transformed into Mach1 *E. coli* and sequenced to confirm integrity. The complement and empty vectors were electroporated into corresponding AB5075 mutant strains. Replication in the AB5075 mutant strains was confirmed by standard PCR.

Twitching Motility Assays

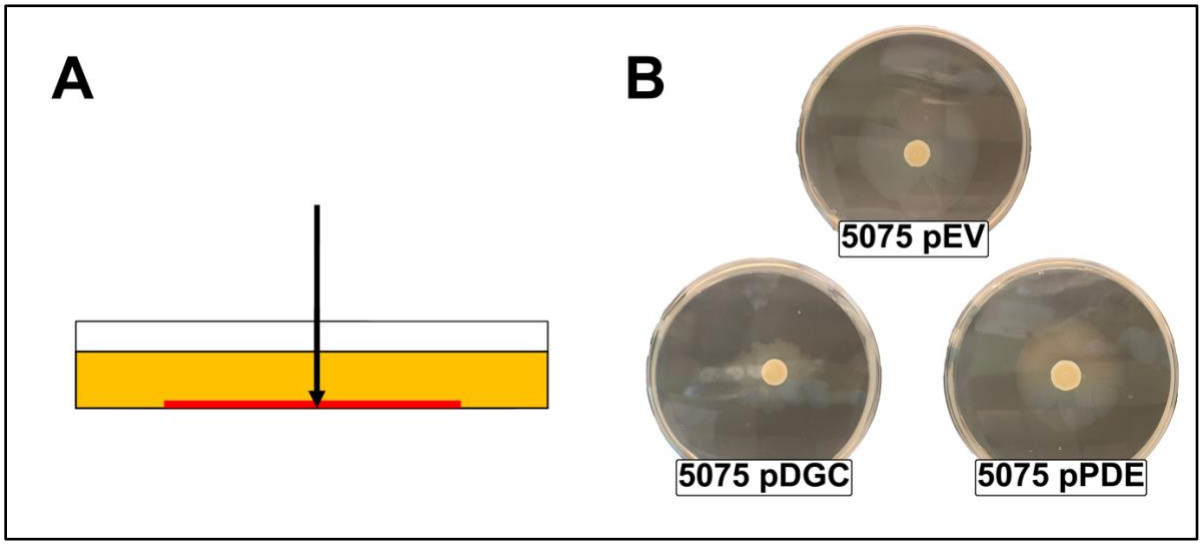

FIG 12. Twitching motility plate inoculation technique

(A) The smaller (top) rectangle is the lid of the dish. The yellow represents the motility medium. The red is the area the bacteria will grow. The black arrow shows the way the bacteria were inoculated by going past the opened lid and through the medium to the plastic bottom of the Petri dish. The plates were stabbed (black arrow) with 2 µL of 1.0 OD_{600} AB5075 transposon mutant cultures and grown 20–24 hours at 37 °C. The bacteria grew (red) in the space between the plastic and the motility medium (yellow). Perpendicular diameters of bacterial growth (red) were measured and averaged.

(B) A few examples of twitching motility plates are shown.

Twitching motility plates were made from LB containing 4.0 g/L powdered Fisher Science Education™ Agar Bacteriological. Twitching motility plates were made the day before experimentation, dried overnight, and used the following day. Bacterial cultures were grown in 2 mL LB medium 20–24 hours to stationary phase. Overnight cultures were diluted to 1.0 OD_{600} in 1.0 mL of LB, and 2 µL of each sample was stabbed through the agar to the plastic of the Petri dish and pipetted out at the bottom while pulling out of the agar medium (FIG 12). These plates were incubated 20–24 hours at 37 °C. The diameter of the distance traveled was measured in two directions perpendicular to one another. Average diameters were calculated, and the normalized values were computed relative to the wild-type strain. The assay was repeated in sextuplicate, and the results were analyzed by paired ANOVA with Dunnett's post hoc test (against a control: wild type) for statistical significance ($p<0.05$) using GraphPad Prism v9.4.0. To perform the complement twitching motility test, the addition of 50 µg/mL rifampicin and 1 mM IPTG to overnight cultures and twitching assay motility plates was done to maintain and induce the pMMB-RIF plasmid, respectively.

Static Biofilm Formation Assays

Overnight cultures of each strain were measured for density by OD_{600} and diluted to 0.05 OD_{600} in LB. 96-well plates were filled with 150 µL of the 0.05 OD_{600} cultures into a column of eight wells as technical replicates. The order of the mutant strains was randomized among trials, to reduce the error generated by disproportionate incubation at the plate edges. These 96-well plates were statically incubated at 37 °C 20–24 hours.

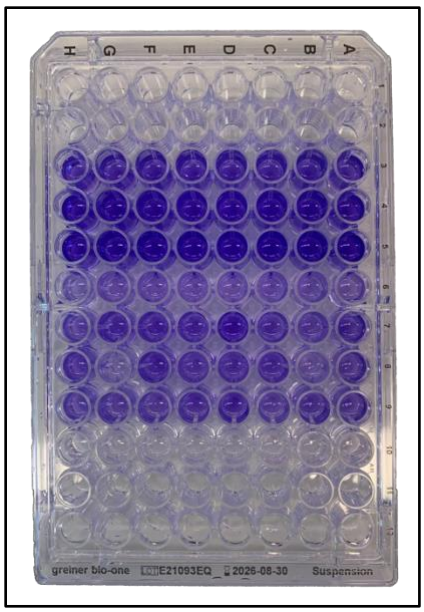

FIG 13. Stained 96-well plate for detection of biofilm

After washing the cultures in distilled water, they are stained in 200 µL of a 0.1 % crystal violet and Milli-Q® ultrapure water solution for fifteen minutes. This is dumped as waste, and the plate was dried. The stained biofilm was resuspended in 200 µL of 95 %–100 % ethanol. At 595 nm, the optical density was determined. As seen in the picture above, the darker purple means that more biofilm adhered to the plastic well walls. Each row was averaged as octuplets (from left to right per the picture) to make a single data point.

After the incubation period, samples were removed, and plates were washed with distilled water. The remaining biofilm in each well was stained with 200 µL of a 0.1 % crystal violet and Milli-Q® ultrapure water solution for fifteen minutes on an automated rocker. After staining was complete, crystal violet was dumped into a waste container, and plates were washed three times with distilled water. Stained 96-well plates were shaken vigorously to expel excess water from the wells and dried in a fume hood with the lid open 2–3 hours. Once dry, crystal violet was resuspended with 200 µL of 95–

100 % ethanol in each well. Plates were placed back on the rocker for five minutes to dissolve the crystal violet on the well walls, and retained crystal violet was measured by OD_{595} in a BioTek Synergy HTX Multimode Reader with Gen5 Microplate Reader and Imager Software (FIG 13). Raw values of each strain were normalized relative to the wild-type strain, which was included as a negative control in each plate. The results were analyzed by ANOVA with Dunnett's post hoc test (against a control: wild type) for statistical significance ($p<0.05$) using GraphPad Prism v9.4.0. To perform the static biofilm formation assay on the complement strains, the same procedures were used for those mutants. Additionally, supplementing the LB medium with 50 µg/mL rifampicin and 1 mM IPTG was done to maintain and induce the pMMB-RIF plasmid, respectively.

Desiccation Tolerance Assays

One milliliter of an overnight LB culture was transferred to a 1.5 mL microcentrifuge tube, centrifuged at max speed for 30 seconds, and washed with autoclaved Milli-Q® ultrapure water three times to remove excess salt and osmolytes. The final pellet was resuspended with Milli-Q® ultrapure water, and its OD_{600} was analyzed. The cultures were diluted in Milli-Q® ultrapure water to 1.0 OD_{600}, vortexed to ensure homogeneity, and 10 µL of the diluted cultures were transferred to a 96-well plate in duplicate. This desiccation plate was placed in a fume hood with the blower on and the lid of the plate off 2–3 hours to ensure the samples were dry. When samples were fully dried, the plate was transferred to an incubator at 25 °C for 48 hours (94).

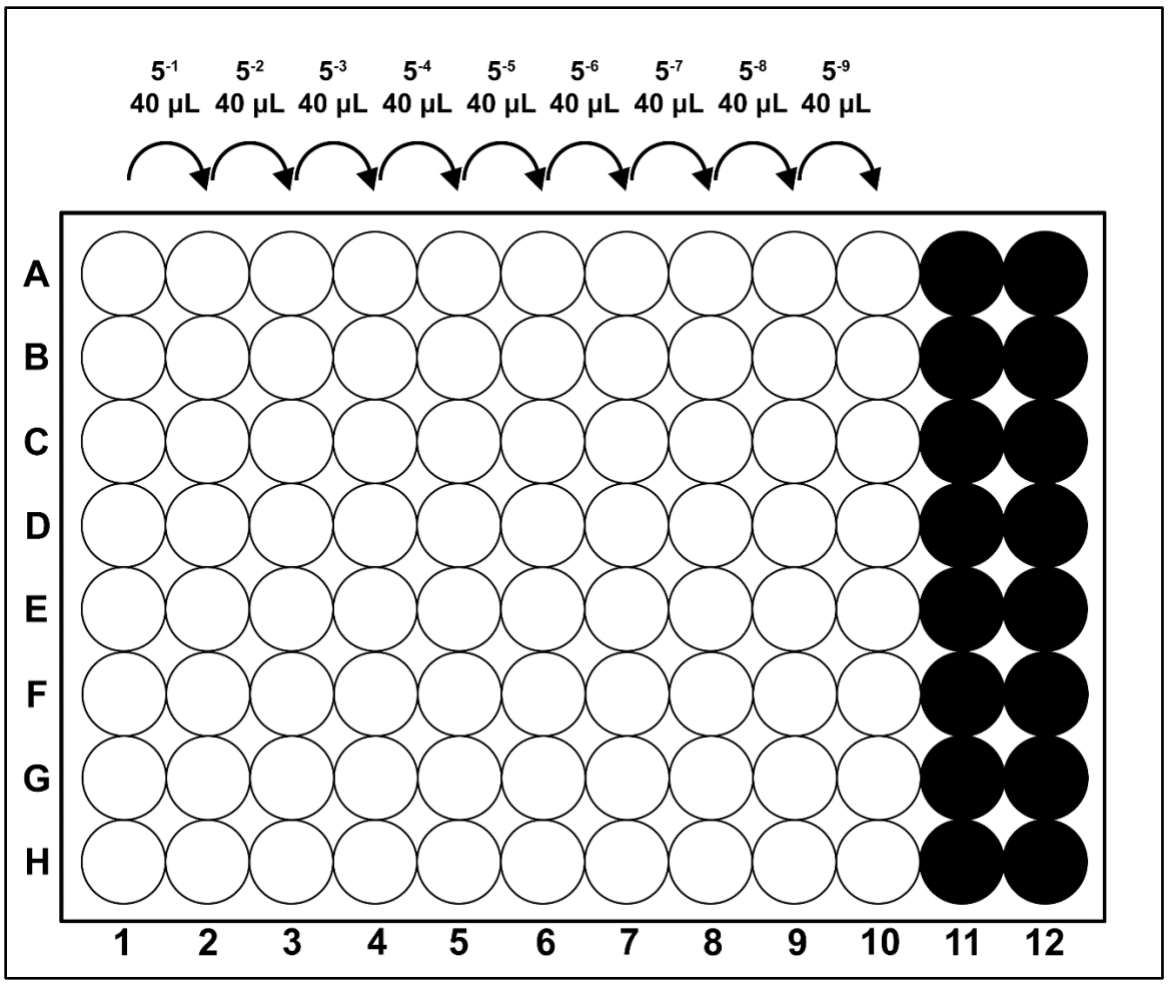

FIG 14. 5-fold serial dilutions in a 96-well plate

160 µL of PBS was put into all wells from columns 1 to 10. Then, 40 µL of 1.0 OD_{600}-diluted overnight cultures of each transposon mutant was placed in the first column of different rows. This diluted the samples by a factor of 5 for each dilution. Samples were pipetted up and down a few times to wash the tips to ensure homogeneity. Tips were discarded, and fresh tips were used to transfer 40 µL from column 1 to 2; this was repeated until column 10 was reached. Columns 11 and 12 (black) are unused.

To determine the starting bacterial concentration applied to the desiccation plates, 1.0 OD_{600}-diluted samples were vortexed again to ensure homogeneity and quantified as previously described (94). In short, 160 µL of PBS was pipetted into all wells from columns 1 to 10. 40 µL of the 1.0 OD_{600} samples were transferred into the first column of a 96-well plate. Samples were serially diluted 1:5 between column 1–10 (FIG 14); then from column 5 to 10, 7 µL of diluted samples were pipetted six times onto a dried 1.5 % agar LB plate (FIG 15). Droplets were allowed to soak into the plates 10–15 minutes and incubated overnight at 25 °C. Once sufficiently countable, CFUs of a single dilution were counted for the inoculum counts.

After two days at 25 °C, the 96-well desiccation plate was removed from the incubator. 200 µL autoclaved Milli-Q® ultrapure water was added to each well, and the desiccation plate was placed on a 96-well plate shaker for 10 minutes at 1000 rpm to rehydrate the samples. Desiccation samples were quantified as described for the inocula. The survival of each strain was determined by converting values to the inoculum's starting concentration. Duplicate survival values of each strain from the desiccation plate were averaged to generate a single data point. The assay was repeated in triplicate, and the results were analyzed by paired ANOVA with Dunnett's post hoc test (against a control: wild type) for statistical significance ($p<0.05$) using GraphPad Prism v9.4.0.

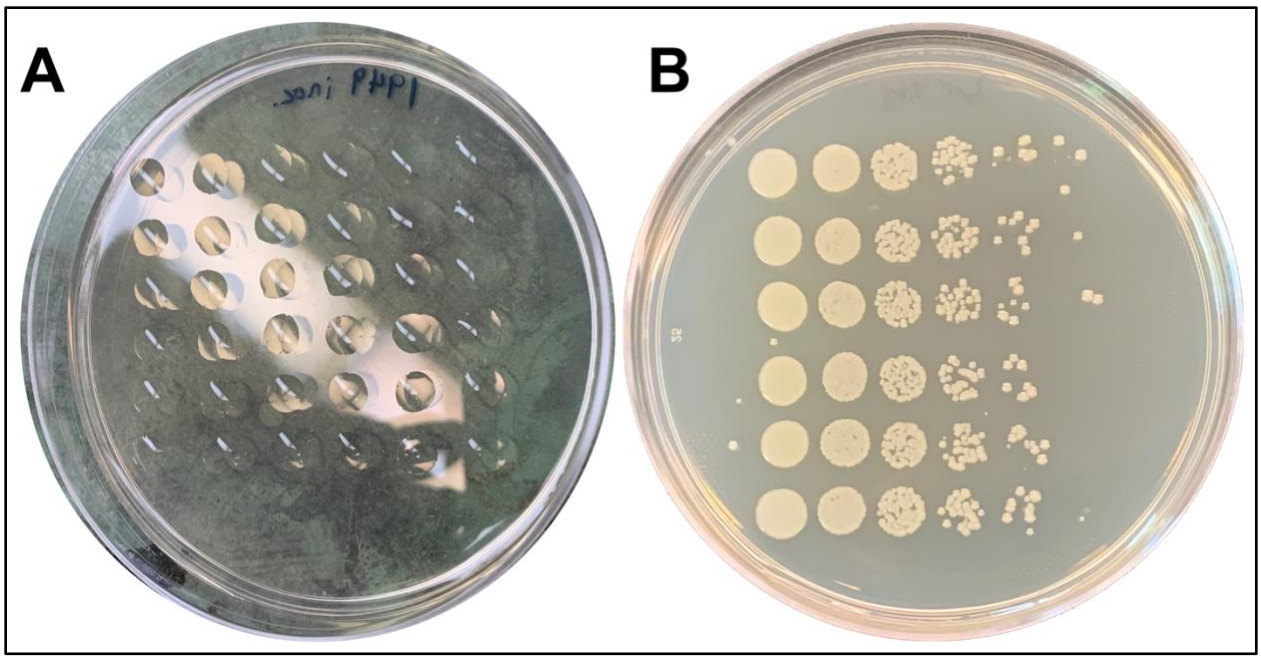

FIG 15. The 6×6 drop plate method for sextuplet CFUs per trial

From left to right, the dilution spots are columns 5–10 from the serially diluted 96-well plate in FIG 14. (A) A representation of the 7 µL 5–10 column onto a dried 1.5% agar LB plate is shown. This 6×6 drop plate method would allow for counting colonies at different dilutions while receiving six technical replicates of counts. (B) Once incubated for 25 °C overnight, CFUs were counted at spots of a single dilution. Countable columns were considered CFU totals between 20 and 100 colonies of a single column (or on average, 3 to 17 colonies in each spot).

REFERENCES

1. Mulani MS, Kamble EE, Kumkar SN, Tawre MS, Pardesi KR. 2019. Emerging strategies to combat ESKAPE pathogens in the era of antimicrobial resistance: a review. Front Microbiol 10:539.
2. Santajit S, Indrawattana N. 2016. Mechanisms of antimicrobial resistance in ESKAPE pathogens. Biomed Res Int 2016:2475067.
3. Llaca-Díaz JM, Mendoza-Olazarán S, Camacho-Ortiz A, Flores S, Garza-González E. 2012. One-year surveillance of ESKAPE pathogens in an intensive care unit of Monterrey, Mexico. Chemotherapy 58:475-81.
4. Benkő R, Gajdács M, Matuz M, Bodó G, Lázár A, Hajdú E, Papfalvi E, Hannauer P, Erdélyi P, Pető Z. 2020. Prevalence and antibiotic resistance of ESKAPE pathogens isolated in the emergency department of a tertiary care teaching hospital in Hungary: a 5-year retrospective survey. Antibiotics (Basel) 9:624.
5. Sharma D, Misba L, Khan AU. 2019. Antibiotics versus biofilm: an emerging battleground in microbial communities. Antimicrob Resist Infect Control 8:76.
6. Chung PY, Toh YS. 2014. Anti-biofilm agents: recent breakthrough against multi-drug resistant Staphylococcus aureus. Pathog Dis 70:231-9.
7. Römling U, Balsalobre C. 2012. Biofilm infections, their resilience to therapy and innovative treatment strategies. J Intern Med 272:541-61.
8. Wu H, Moser C, Wang HZ, Høiby N, Song ZJ. 2015. Strategies for combating bacterial biofilm infections. Int J Oral Sci 7:1-7.
9. Zimmerli W, Lew PD, Waldvogel FA. 1984. Pathogenesis of foreign body infection. Evidence for a local granulocyte defect. J Clin Invest 73:1191-200.
10. Tacconelli E, Magrini N, Weyer K, Hill S, Raviglione M. 2017. Prioritization of pathogens to guide discovery, research and development of new antibiotics for drug-resistant bacterial infections, including tuberculosis. Geneva: World Health Organization (WHO/EMP/IAU/2017.12):39-82.
11. Gashaw M, Berhane M, Bekele S, Kibru G, Teshager L, Yilma Y, Ahmed Y, Fentahun N, Assefa H, Wieser A, Gudina EK, Ali S. 2018. Emergence of high drug resistant bacterial isolates from patients with health care associated

infections at Jimma University medical center: a cross sectional study. Antimicrob Resist Infect Control 7:138.

12. Kołpa M, Wałaszek M, Gniadek A, Wolak Z, Dobroś W. 2018. Incidence, microbiological profile and risk factors of healthcare-associated infections in intensive care units: a 10 year observation in a provincial hospital in southern Poland. Int J Environ Res Public Health 15:112.
13. Matta R, Hallit S, Hallit R, Bawab W, Rogues AM, Salameh P. 2018. Epidemiology and microbiological profile comparison between community and hospital acquired infections: a multicenter retrospective study in Lebanon. J Infect Public Health 11:405-411.
14. Manchanda V, Sanchaita S, Singh N. 2010. Multidrug resistant Acinetobacter. J Glob Infect Dis 2:291-304.
15. Farrow JM, Wells G, Pesci EC. 2018. Desiccation tolerance in Acinetobacter baumannii is mediated by the two-component response regulator BfmR. PLoS One 13:e0205638.
16. Jacobs AC, Thompson MG, Black CC, Kessler JL, Clark LP, McQueary CN, Gancz HY, Corey BW, Moon JK, Si Y, Owen MT, Hallock JD, Kwak YI, Summers A, Li CZ, Rasko DA, Penwell WF, Honnold CL, Wise MC, Waterman PE, Lesho EP, Stewart RL, Actis LA, Palys TJ, Craft DW, Zurawski DV. 2014. AB5075, a highly virulent isolate of Acinetobacter baumannii, as a model strain for the evaluation of pathogenesis and antimicrobial treatments. mBio 5:e01076-14.
17. Tipton KA, Rather PN. 2017. An ompR–envZ two-component system ortholog regulates phase variation, osmotic tolerance, motility, and virulence in Acinetobacter baumannii strain AB5075. J Bacteriol 199:e00705-16.
18. Dijkshoorn L, Nemec A, Seifert H. 2007. An increasing threat in hospitals: multidrug-resistant Acinetobacter baumannii. Nat Rev Microbiol 5:939-51.
19. Pourakbari B, Mahmoudi S, Habibi R, Ashtiani MTH, Sadeghi RH, Khodabandeh M, Mamishi S. 2018. An increasing threat in an Iranian referral children's hospital: multidrug-resistant Acinetobacter baumannii. Infect Disord Drug Targets 18:129-135.

20. Bradley DE. 1972. Shortening of Pseudomonas aeruginosa pili after RNA-phage adsorption. J Gen Microbiol 72:303-19.
21. Jacobsen T, Bardiaux B, Francetic O, Izadi-Pruneyre N, Nilges M. 2020. Structure and function of minor pilins of type IV pili. Med Microbiol Immunol 209:301-8.
22. Cehovin A, Winterbotham M, Lucidarme J, Borrow R, Tang CM, Exley RM, Pelicic V. 2010. Sequence conservation of pilus subunits in Neisseria meningitidis. Vaccine 28:4817-26.
23. Mattick JS. 2002. Type IV pili and twitching motility. Annu Rev Microbiol 56:289-314.
24. Antunes LC, Imperi F, Carattoli A, Visca P. 2011. Deciphering the multifactorial nature of Acinetobacter baumannii pathogenicity. PLoS One 6:e22674.
25. Akrami F, Namvar AE. 2019. Acinetobacter baumannii as nosocomial pathogenic bacteria. Mol Gen Microbiol Virol 34:84-96.
26. Harding CM, Tracy EN, Carruthers MD, Rather PN, Actis LA, Munson RS. 2013. Acinetobacter baumannii strain M2 produces type IV pili which play a role in natural transformation and twitching motility but not surface-associated motility. mBio 4:e00360-13.
27. Ronish LA, Lillehoj E, Fields JK, Sundberg EJ, Piepenbrink KH. 2019. The structure of PilA from Acinetobacter baumannii AB5075 suggests a mechanism for functional specialization in Acinetobacter type IV pili. J Biol Chem 294:218-30.
28. Pakharukova N, Tuittila M, Paavilainen S, Malmi H, Parilova O, Teneberg S, Knight SD, Zavialov AV. 2018. Structural basis for Acinetobacter baumannii biofilm formation. Proc Natl Acad Sci U S A 115:5558-63.
29. Chen CL, Dudek A, Liang YH, Janapatla RP, Lee HY, Hsu L, Kuo HY, Chiu CH. 2022. D-mannose-sensitive pilus of Acinetobacter baumannii is linked to biofilm formation and adherence onto respiratory tract epithelial cells. J Microbiol Immunol Infect 55:69-79.
30. Wimpenny J, Manz W, Szewzyk U. 2000. Heterogeneity in biofilms. FEMS Microbiol Rev 24:661-71.

31. Yoshida K, Matsumoto T, Tateda K, Uchida K, Tsujimoto S, Yamaguchi K. 2000. Role of bacterial capsule in local and systemic inflammatory responses of mice during pulmonary infection with Klebsiella pneumoniae. J Med Microbiol 49:1003-10.
32. Stollerman GH, Dale JB. 2008. The importance of the group A Streptococcus capsule in the pathogenesis of human infections: a historical perspective. Clin Infect Dis 46:1038-45.
33. Hunter P. 2008. The mob response. The importance of biofilm research for combating chronic diseases and tackling contamination. EMBO Rep 9:314-7.
34. Rabin N, Zheng Y, Opoku-Temeng C, Du Y, Bonsu E, Sintim HO. 2015. Biofilm formation mechanisms and targets for developing antibiofilm agents. Future Med Chem 7:493-512.
35. Itoh Y, Rice JD, Goller C, Pannuri A, Taylor J, Meisner J, Beveridge TJ, Preston JF, Romeo T. 2008. Roles of pgaABCD genes in synthesis, modification, and export of the Escherichia coli biofilm adhesin poly-β-1,6-N-acetyl-D-glucosamine. J Bacteriol 190:3670-80.
36. Wang X, Preston JF, Romeo T. 2004. The pgaABCD locus of Escherichia coli promotes the synthesis of a polysaccharide adhesin required for biofilm formation. J Bacteriol 186:2724-34.
37. Zielinski NA, Chakrabarty AM, Berry A. 1991. Characterization and regulation of the Pseudomonas aeruginosa algC gene encoding phosphomannomutase. J Biol Chem 266:9754-63.
38. Alkawash MA, Soothill JS, Schiller NL. 2006. Alginate lyase enhances antibiotic killing of mucoid Pseudomonas aeruginosa in biofilms. Acta Pathol Microbiol Immunol Scandinavica (APMIS) 114:131-8.
39. Charlesworth CJ, Saran VV, K. VL, Woods HL. 2008. The role of biofilm structure in the mechanism of gentamicin and ciprofloxacin antibiotic resistance in P. aeruginosa PAO1 biofilms. J Experimental Microbiol and Immunol 12:27-33.
40. Peñaloza-Vázquez A, Fakhr MK, Bailey AM, Bender CL. 2004. AlgR functions in algC expression and virulence in Pseudomonas syringae pv. syringae. Microbiology (Reading) 150:2727-37.

41. Shankar S, Ye RW, Schlictman D, Chakrabarty AM. 1995. Exopolysaccharide alginate synthesis in Pseudomonas aeruginosa: enzymology and regulation of gene expression. Adv Enzymol Relat Areas Mol Biol 70:221-55.
42. Oda Y, Shapiro MM, Lewis NM, Zhong X, Huse HK, Zhong W, Bruce JE, Manoil C, Harwood CS. 2022. CsrA-controlled proteins reveal new dimensions of Acinetobacter baumannii desiccation tolerance. J Bacteriol 204:e0047921.
43. Jawad A, Heritage J, Snelling AM, Gascoyne-Binzi DM, Hawkey PM. 1996. Influence of relative humidity and suspending menstrua on survival of Acinetobacter spp. on dry surfaces. J Clin Microbiol 34:2881-7.
44. Guttenplan SB, Kearns DB. 2013. Regulation of flagellar motility during biofilm formation. FEMS Microbiol Rev 37:849-71.
45. Trimble MJ, McCarter LL. 2011. Bis-(3'-5')-cyclic dimeric GMP-linked quorum sensing controls swarming in Vibrio parahaemolyticus. Proc Natl Acad Sci U S A 108:18079-84.
46. Huang B, Whitchurch CB, Mattick JS. 2003. FimX, a multidomain protein connecting environmental signals to twitching motility in Pseudomonas aeruginosa. J Bacteriol 185:7068-76.
47. Ahmad I, Nygren E, Khalid F, Myint SL, Uhlin BE. 2020. A cyclic-di-GMP signalling network regulates biofilm formation and surface associated motility of Acinetobacter baumannii 17978. Sci Rep 10:1991.
48. Schäper S, Krol E, Skotnicka D, Kaever V, Hilker R, Søgaard-Andersen L, Becker A. 2016. Cyclic di-GMP regulates multiple cellular functions in the symbiotic Alphaproteobacterium Sinorhizobium meliloti. J Bacteriol 198:521-35.
49. Abel S, Bucher T, Nicollier M, Hug I, Kaever V, Abel Zur Wiesch P, Jenal U. 2013. Bi-modal distribution of the second messenger c-di-GMP controls cell fate and asymmetry during the Caulobacter cell cycle. PLoS Genet 9:e1003744.
50. Hallberg ZF, Chan CH, Wright TA, Kranzusch PJ, Doxzen KW, Park JJ, Bond DR, Hammond MC. 2019. Structure and mechanism of a Hypr GGDEF enzyme that activates cGAMP signaling to control extracellular metal respiration. Elife 8:e43959.

51. Ueda A, Wood TK. 2009. Connecting quorum sensing, c-di-GMP, pel polysaccharide, and biofilm formation in Pseudomonas aeruginosa through tyrosine phosphatase TpbA (PA3885). PLoS Pathog 5:e1000483.
52. Marvig RL, Sommer LM, Molin S, Johansen HK. 2015. Convergent evolution and adaptation of Pseudomonas aeruginosa within patients with cystic fibrosis. Nat Genet 47:57-64.
53. Chan C, Paul R, Samoray D, Amiot NC, Giese B, Jenal U, Schirmer T. 2004. Structural basis of activity and allosteric control of diguanylate cyclase. Proc Natl Acad Sci U S A 101:17084-9.
54. Tchigvintsev A, Xu X, Singer A, Chang C, Brown G, Proudfoot M, Cui H, Flick R, Anderson WF, Joachimiak A, Galperin MY, Savchenko A, Yakunin AF. 2010. Structural insight into the mechanism of c-di-GMP hydrolysis by EAL domain phosphodiesterases. J Mol Biol 402:524-38.
55. Rao F, Yang Y, Qi Y, Liang ZX. 2008. Catalytic mechanism of cyclic di-GMP–specific phosphodiesterase: a study of the EAL domain-containing RocR from Pseudomonas aeruginosa. J Bacteriol 190:3622-31.
56. Robert-Paganin J, Nonin-Lecomte S, Réty S. 2012. Crystal structure of an EAL domain in complex with reaction product 5'-pGpG. PLoS One 7:e52424.
57. Römling U. 2009. Rationalizing the evolution of EAL domain-based cyclic di-GMP-specific phosphodiesterases. J Bacteriol 191:4697-700.
58. Tamayo R, Tischler AD, Camilli A. 2005. The EAL domain protein VieA is a cyclic diguanylate phosphodiesterase. J Biol Chem 280:33324-30.
59. Ferreira RB, Antunes LC, Greenberg EP, McCarter LL. 2008. Vibrio parahaemolyticus ScrC modulates cyclic dimeric GMP regulation of gene expression relevant to growth on surfaces. J Bacteriol 190:851-60.
60. Christen M, Christen B, Folcher M, Schauerte A, Jenal U. 2005. Identification and characterization of a cyclic di-GMP–specific phosphodiesterase and its allosteric control by GTP. J Biol Chem 280:30829-37.
61. Bordeleau E, Fortier LC, Malouin F, Burrus V. 2011. C-di-GMP turn-over in Clostridium difficile is controlled by a plethora of diguanylate cyclases and phosphodiesterases. PLoS Genet 7:e1002039.

62. Hinsa SM, O'Toole GA. 2006. Biofilm formation by Pseudomonas fluorescens WCS365: a role for LapD. Microbiology (Reading) 152:1375-83.
63. Schmidt AJ, Ryjenkov DA, Gomelsky M. 2005. The ubiquitous protein domain EAL is a cyclic diguanylate-specific phosphodiesterase: enzymatically active and inactive EAL domains. J Bacteriol 187:4774-81.
64. Alm RA, Bodero AJ, Free PD, Mattick JS. 1996. Identification of a novel gene, pilZ, essential for type 4 fimbrial biogenesis in Pseudomonas aeruginosa. J Bacteriol 178:46-53.
65. Ryan RP, Tolker-Nielsen T, Dow JM. 2012. When the PilZ don't work: effectors for cyclic di-GMP action in bacteria. Trends Microbiol 20:235-42.
66. Pultz IS, Christen M, Kulasekara HD, Kennard A, Kulasekara B, Miller SI. 2012. The response threshold of Salmonella PilZ domain proteins is determined by their binding affinities for c-di-GMP. Mol Microbiol 86:1424-40.
67. Ryjenkov DA, Simm R, Römling U, Gomelsky M. 2006. The PilZ domain is a receptor for the second messenger c-di-GMP: the PilZ domain protein YcgR controls motility in enterobacteria. J Biol Chem 281:30310-4.
68. Amikam D, Galperin MY. 2006. PilZ domain is part of the bacterial c-di-GMP binding protein. Bioinformatics 22:3-6.
69. McCarthy Y, Ryan RP, O'Donovan K, He YQ, Jiang BL, Feng JX, Tang JL, Dow JM. 2008. The role of PilZ domain proteins in the virulence of Xanthomonas campestris pv. campestris. Mol Plant Pathol 9:819-24.
70. Guzzo CR, Salinas RK, Andrade MO, Farah CS. 2009. PilZ protein structure and interactions with PilB and the FimX EAL domain: implications for control of type IV pilus biogenesis. J Mol Biol 393:848-66.
71. Paul K, Nieto V, Carlquist WC, Blair DF, Harshey RM. 2010. The c-di-GMP binding protein YcgR controls flagellar motor direction and speed to affect chemotaxis by a "backstop brake" mechanism. Mol Cell 38:128-39.
72. Pendleton JN, Gorman SP, Gilmore BF. 2013. Clinical relevance of the ESKAPE pathogens. Expert Rev Anti Infect Ther 11:297-308.

73. Paul R, Weiser S, Amiot NC, Chan C, Schirmer T, Giese B, Jenal U. 2004. Cell cycle-dependent dynamic localization of a bacterial response regulator with a novel di-guanylate cyclase output domain. Genes Dev 18:715-27.
74. Ueda A, Wood TK. 2010. Tyrosine phosphatase TpbA of Pseudomonas aeruginosa controls extracellular DNA via cyclic diguanylic acid concentrations. Environ Microbiol 2:449-55.
75. Schultz J, Milpetz F, Bork P, Ponting CP. 1998. SMART, a simple modular architecture research tool: identification of signaling domains. Proc Natl Acad Sci U S A 95:5857-64.
76. Marchler-Bauer A, Lu S, Anderson JB, Chitsaz F, Derbyshire MK, DeWeese-Scott C, Fong JH, Geer LY, Geer RC, Gonzales NR, Gwadz M, Hurwitz DI, Jackson JD, Ke Z, Lanczycki CJ, Lu F, Marchler GH, Mullokandov M, Omelchenko MV, Robertson CL, Song JS, Thanki N, Yamashita RA, Zhang D, Zhang N, Zheng C, Bryant SH. 2011. CDD: a Conserved Domain Database for the functional annotation of proteins. Nucleic Acids Res 39:D225-9.
77. Su J, Zou X, Huang L, Bai T, Liu S, Yuan M, Chou SH, He YW, Wang H, He J. 2016. DgcA, a diguanylate cyclase from Xanthomonas oryzae pv. oryzae regulates bacterial pathogenicity on rice. Sci Rep 6:25978.
78. Gallagher LA, Ramage E, Weiss EJ, Radey M, Hayden HS, Held KG, Huse HK, Zurawski DV, Brittnacher MJ, Manoil C. 2015. Resources for genetic and genomic analysis of emerging pathogen Acinetobacter baumannii. J Bacteriol 197:2027-35.
79. Clark DP, Pazdernik NJ. 2013. Regulation of transcription in prokaryotes. Molecular Biology 2(ed):e338-43.
80. Karalewitz AP, Miller SI. 2018. Multidrug-resistant Acinetobacter baumannii chloramphenicol resistance requires an inner membrane permease. Antimicrob Agents Chemother 62:e00513-18.
81. Clemmer KM, Bonomo RA, Rather PN. 2011. Genetic analysis of surface motility in Acinetobacter baumannii. Microbiology (Reading) 157:2534-44.
82. Mayer C, Muras A, Parga A, Romero M, Rumbo-Feal S, Poza M, Ramos-Vivas J, Otero A. 2020. Quorum sensing as a target for controlling surface associated

motility and biofilm formation in Acinetobacter baumannii ATCC® 17978™. Front Microbiol 11:565548.

83. Sun X, Ni Z, Tang J, Ding Y, Wang X, Li F. 2021. The abaI/abaR quorum-sensing system effects on pathogenicity in Acinetobacter baumannii. Front Microbiol 12:679241.
84. Mussi MA, Gaddy JA, Cabruja M, Arivett BA, Viale AM, Rasia R, Actis LA. 2010. The opportunistic human pathogen Acinetobacter baumannii senses and responds to light. J Bacteriol 192:6336-45.
85. Wood CR, Ohneck EJ, Edelmann RE, Actis LA. 2018. A light-regulated type I pilus contributes to Acinetobacter baumannii biofilm, motility, and virulence functions. Infect Immun 86:e00442-18.
86. Eijkelkamp BA, Hassan KA, Paulsen IT, Brown MH. 2011. Investigation of the human pathogen Acinetobacter baumannii under iron limiting conditions. BMC Genomics 12:126.
87. Wang X, Dubey AK, Suzuki K, Baker CS, Babitzke P, Romeo T. 2005. CsrA post-transcriptionally represses pgaABCD, responsible for synthesis of a biofilm polysaccharide adhesin of Escherichia coli. Mol Microbiol 56:1648-63.
88. Galperin MY, Chou SH. 2020. Structural conservation and diversity of PilZ-related domains. J Bacteriol 202:e00664-19.
89. Chen LH, Köseoğlu VK, Güvener ZT, Myers-Morales T, Reed JM, D'Orazio SE, Miller KW, Gomelsky M. 2014. Cyclic di-GMP–dependent signaling pathways in the pathogenic Firmicute Listeria monocytogenes. PLoS Pathog 10:e1004301.
90. Martínez-Ortiz IC, Ahumada-Manuel CL, Hsueh BY, Guzmán J, Moreno S, Cocotl-Yañez M, Waters CM, Zamorano-Sánchez D, Espín G, Núñez C. 2020. Cyclic di-GMP–mediated regulation of extracellular mannuronan C-5 epimerases is essential for cyst formation in Azotobacter vinelandii. J Bacteriol 202:e00135-20.
91. Whitney JC, Whitfield GB, Marmont LS, Yip P, Neculai AM, Lobsanov YD, Robinson H, Ohman DE, Howell PL. 2015. Dimeric c-di-GMP is required for post-translational regulation of alginate production in Pseudomonas aeruginosa. J Biol Chem 290:12451-62.

92. Merighi M, Lee VT, Hyodo M, Hayakawa Y, Lory S. 2007. The second messenger bis-(3'-5')-cyclic-GMP and its PilZ domain-containing receptor Alg44 are required for alginate biosynthesis in Pseudomonas aeruginosa. Mol Microbiol 65:876-95.
93. Gibson DG, Young L, Chuang RY, Venter JC, Hutchison CA, Smith HO. 2009. Enzymatic assembly of DNA molecules up to several hundred kilobases. Nat Methods 6:343-5.
94. Chen CY, Nace GW, Irwin PL. 2003. A 6 x 6 drop plate method for simultaneous colony counting and MPN enumeration of Campylobacter jejuni, Listeria monocytogenes, and Escherichia coli. J Microbiol Methods 55:475-9.
95. Figurski DH, Helinski DR. 1979. Replication of an origin-containing derivative of plasmid RK2 dependent on a plasmid function provided in trans. Proc Natl Acad Sci U S A 76:1648-52.
96. Knauf VC, Nester EW. 1982. Wide host range cloning vectors: a cosmid clone bank of an Agrobacterium Ti plasmid. Plasmid 8:45-54.
97. Hoang TT, Karkhoff-Schweizer RR, Kutchma AJ, Schweizer HP. 1998. A broad-host-range Flp-FRT recombination system for site-specific excision of chromosomally-located DNA sequences: application for isolation of unmarked Pseudomonas aeruginosa mutants. Gene 212:77-86.
98. Datsenko KA, Wanner BL. 2000. One-step inactivation of chromosomal genes in Escherichia coli K-12 using PCR products. Proc Natl Acad Sci U S A 97:6640-5.
99. Baumann P, Doudoroff M, Stanier RY. 1968. A study of the Moraxella group. II. oxidative-negative species (genus Acinetobacter). J Bacteriol 95:1520-41.
100. Smith MG, Gianoulis TA, Pukatzki S, Mekalanos JJ, Ornston LN, Gerstein M, Snyder M. 2007. New insights into Acinetobacter baumannii pathogenesis revealed by high-density pyrosequencing and transposon mutagenesis. Genes Dev 21:601-14.
101. Kearns DB. 2010. A field guide to bacterial swarming motility. Nat Rev Microbiol 8:634-44.
102. Blaschke U, Skiebe E, Wilharm G. 2021. Novel genes required for surface-associated motility in Acinetobacter baumannii. Curr Microbiol 78:1509-28.

103. Caiazza NC, Shanks RM, O'Toole GA. 2005. Rhamnolipids modulate swarming motility patterns of Pseudomonas aeruginosa. J Bacteriol 187:7351-61.
104. Pérez-Varela M, Tierney ARP, Kim JS, Vázquez-Torres A, Rather P. 2020. Characterization of RelA in Acinetobacter baumannii. J Bacteriol 202:e00045-20.
105. McQueary CN, Kirkup BC, Si Y, Barlow M, Actis LA, Craft DW, Zurawski DV. 2012. Extracellular stress and lipopolysaccharide modulate Acinetobacter baumannii surface-associated motility. J Microbiol 50:434-43.
106. Skiebe E, de Berardinis V, Morczinek P, Kerrinnes T, Faber F, Lepka D, Hammer B, Zimmermann O, Ziesing S, Wichelhaus TA, Hunfeld KP, Borgmann S, Gröbner S, Higgins PG, Seifert H, Busse HJ, Witte W, Pfeifer Y, Wilharm G. 2012. Surface-associated motility, a common trait of clinical isolates of Acinetobacter baumannii, depends on 1,3-diaminopropane. Int J Med Microbiol 302:117-28.
107. Lin L, Zhou M, Shen D, Han S, Fulano AM, Chou S, Qian G. 2020. A non-flagellated biocontrol bacterium employs a PilZ-PilB complex to provoke twitching motility associated with its predation behavior. Phytopathol Res 2:12.
108. Steinmetz M, Le Coq D, Djemia HB, Gay P. 1983. [Genetic analysis of sacB, the structural gene of a secreted enzyme, levansucrase of Bacillus subtilis Marburg]. Mol Gen Genet 191:138-44.

APPENDICES

Appendix A. Strains Used in This Study

Strain	Genotype	Source
17978	Wild-type *Acinetobacter baumannii* Bouvet and Grimont (ATCC® 17978™)	ATCC®
AB5075-UW	Wild-type *Acinetobacter baumannii* str. AB5075	(16)
E. coli Mach1™	*E. coli* str. W *ΔrecA1398 endA1 fhuA Φ*80*Δ*(*lac*)M15 *Δ*(*lac*)*X74 hsdR*($r_K^-m_K^+$)	Invitrogen™
AB00389	AB5075 ABUW_0137(*dgc1*)::Tn*26*(Tet^R)	This study
AB00520	AB5075 ABUW_0188(*dgc2*)::Tn*26*(Tet^R)	This study
AB00844	AB5075 ABUW_0304(*pilA*)::Tn*26*(Tet^R)	This study
AB01347	AB5075 ABUW_0506(*dgc3*)::Tn*26*(Tet^R)	This study
AB02822	AB5075 ABUW_1045(*dgc4*)::Tn*26*(Tet^R)	This study
AB03095	AB5075 ABUW_1138(*dgc5*)::Tn*26*(Tet^R)	This study
AB03312	AB5075 ABUW_1221(*dce1*)::Tn*26*(Tet^R)	This study
AB03972	AB5075 ABUW_1488(*csuA*)::Tn*26*(Tet^R)	This study
AB04138	AB5075 ABUW_1557(*pgaA*)::Tn*26*(Tet^R)	This study
AB04621	AB5075 ABUW_1764(*dce2*)::Tn*26*(Tet^R)	This study
AB05592	AB5075 ABUW_2135(*dgc5*)::Tn*26*(Tet^R)	This study
AB05915	AB5075 ABUW_2255(*cbe1*)::Tn*26*(Tet^R)	This study
AB07393	AB5075 ABUW_2824(*dgc6*)::Tn*26*(Tet^R)	This study
AB08001	AB5075 ABUW_3041(*algC*)::Tn*26*(Tet^R)	This study
AB08293	AB5075 ABUW_3178(*dgc7*)::Tn*26*(Tet^R)	This study
AB08769	AB5075 ABUW_3354(*dce3*)::Tn*26*(Tet^R)	This study
GRAB022	AB5075 / pMMB-RIF	This study
GRAB078	AB5075 / PA2133(+PDE)	This study
GRAB079	AB5075 / PA3702(+DGC)	This study
GRAB038	AB5075 ABUW_0137(*dgc1*)::Tn*26*(Tet^R) / pEP382	This study
GRAB035	AB5075 ABUW_0137(*dgc1*)::Tn*26*(Tet^R) / pMMB-RIF	This study
GRAB023	AB5075 ABUW_0188(*dgc2*)::Tn*26*(Tet^R) / pGR016	This study
GRAB024	AB5075 ABUW_0188(*dgc2*)::Tn*26*(Tet^R) / pMMB-RIF	This study
GRAB025	AB5075 ABUW_0506(*dgc3*)::Tn*26*(Tet^R) / pGR017	This study
GRAB026	AB5075 ABUW_0506(*dgc3*)::Tn*26*(Tet^R) / pMMB-RIF	This study

Strain	Genotype	Source
GRAB027	AB5075 ABUW_1045(*dgc4*)::Tn*26*(Tet^R) / pGR018	This study
GRAB028	AB5075 ABUW_1045(*dgc4*)::Tn*26*(Tet^R) / pMMB-RIF	This study
GRAB029	AB5075 ABUW_1138(*dgc5*)::Tn*26*(Tet^R) / pGR019	This study
GRAB030	AB5075 ABUW_1138(*dgc5*)::Tn*26*(Tet^R) / pMMB-RIF	This study
GRAB053	AB5075 ABUW_1221(*dce1*)::Tn*26*(Tet^R) / pEP434	This study
GRAB075	AB5075 ABUW_1221(*dce1*)::Tn*26*(Tet^R) / pMMB-RIF	This study
GRAB031	AB5075 ABUW_1764(*dce2*)::Tn*26*(Tet^R) / pGR020	This study
GRAB032	AB5075 ABUW_1764(*dce2*)::Tn*26*(Tet^R) / pMMB-RIF	This study
GRAB033	AB5075 ABUW_2135(*dgc5*)::Tn*26*(Tet^R) / pGR021	This study
GRAB034	AB5075 ABUW_2135(*dgc5*)::Tn*26*(Tet^R) / pMMB-RIF	This study
GRAB035	AB5075 ABUW_2255(*cbe1*)::Tn*26*(Tet^R) / pGR022	This study
GRAB036	AB5075 ABUW_2255(*cbe1*)::Tn*26*(Tet^R) / pMMB-RIF	This study
GShAB001	AB5075 ABUW_2824(*dgc6*)::Tn*26*(Tet^R) / pGSh001	This study
GShAB002	AB5075 ABUW_2824(*dgc6*)::Tn*26*(Tet^R) / pMMB-RIF	This study
GRAB039	AB5075 ABUW_3178(*dgc7*)::Tn*26*(Tet^R) / pEP380	This study
GRAB036	AB5075 ABUW_3178(*dgc7*)::Tn*26*(Tet^R) / pMMB-RIF	This study
GRAB040	AB5075 ABUW_3354(*dce3*)::Tn*26*(Tet^R) / pEP440	This study
GRAB037	AB5075 ABUW_3354(*dce3*)::Tn*26*(Tet^R) / pMMB-RIF	This study
GRAB007	17978 *Δ*A1S_0490(*cbe2*)::*kan*	This study
GRAB008	17978 *Δ*A1S_0546(*dce3*)::*kan*	This study
GRAB009	17978 *Δ*A1S_0751(*dgc7*)::*kan*	This study
GRAB010	17978 *Δ*A1S_1067(*dgc6*)::*kan*	This study
GRAB011	17978 *Δ*A1S_1254(*pde2*)::*kan*	This study
GRAB012	17978 *Δ*A1S_1559(*cbe1*)::*kan*	This study
GRAB013	17978 *Δ*A1S_1695(*dgc5*)::*kan*	This study
GRAB014	17978 *Δ*A1S_1949(*dce2*)::*kan*	This study
GRAB015	17978 *Δ*A1S_2337(*dce1*)::*kan*	This study
GRAB016	17978 *Δ*A1S_2422(*pde1*)::*kan*	This study
GRAB017	17978 *Δ*A1S_2506(*dgc4*)::*kan*	This study
GRAB018	17978 *Δ*A1S_2986(*dgc3*)::*kan*	This study
GRAB019	17978 *Δ*A1S_3177(*pilA*)::*kan*	This study
GRAB020	17978 *Δ*A1S_3296(*dgc2*)::*kan*	This study
GRAB021	17978 *Δ*A1S_3345(*dgc1*)::*kan*	This study
GRAB054	17978 / pMMB-RIF	This study
GRAB080	17978 / PA2133(+PDE)	This study
GRAB081	17978 / PA3702(+DGC)	This study

Strain	Genotype	Source
GRAB041	17978 *Δ*A1S_1067(*dgc6*)::*kan* / pMMB-RIF	This study
GRAB042	17978 *Δ*A1S_1067(*dgc6*)::*kan* / pGSh001	This study
GRAB043	17978 *Δ*A1S_1254(*pde2*)::*kan* / pMMB-RIF	This study
GRAB044	17978 *Δ*A1S_1254(*pde2*)::*kan* / pGR023	This study
GRAB045	17978 *Δ*A1S_1559(*cbe1*)::*kan* / pMMB-RIF	This study
GRAB046	17978 *Δ*A1S_1559(*cbe1*)::*kan* / pGR022	This study
GRAB047	17978 *Δ*A1S_1695(*dgc5*)::*kan* / pMMB-RIF	This study
GRAB048	17978 *Δ*A1S_1695(*dgc5*)::*kan* / pGR021	This study
GRAB049	17978 *Δ*A1S_2506(*dgc4*)::*kan* / pMMB-RIF	This study
GRAB050	17978 *Δ*A1S_2506(*dgc4*)::*kan* / pGR018	This study
GRAB051	17978 *Δ*A1S_3345(*dgc1*)::*kan* / pMMB-RIF	This study
GRAB052	17978 *Δ*A1S_3345(*dgc1*)::*kan* / pEP382	This study

Appendix B. Plasmids Used in This Study

Name	Vector	Features[a]	Source
pMMB-RIF	pMMB67EH-RIF	RIF	(80)
pEP432	pMMB-RIF-PA2133(PDE)	RIF	This study
pEP433	pMMB-RIF-PA3702(DGC)	RIF	This study
pRK2013		KAN	(95, 96)
pEX18Gm		GEN/SB	(97)
pKD4		KAN	(98)
pGR001	pEX18Gm-A1S_490(*cbe2*)KO-*kan*	KAN/GEN/SB	This study
pGR002	pEX18Gm-A1S_546(*dce3*)KO-*kan*	KAN/GEN/SB	This study
pGR003	pEX18Gm-A1S_751(*dgc7*)KO-*kan*	KAN/GEN/SB	This study
pGR004	pEX18Gm-A1S_1067(*dgc6*)KO-*kan*	KAN/GEN/SB	This study
pGR005	pEX18Gm-A1S_1254(*pde2*)KO-*kan*	KAN/GEN/SB	This study
pGR006	pEX18Gm-A1S_1559(*cbe1*)KO-*kan*	KAN/GEN/SB	This study
pGR007	pEX18Gm-A1S_1695(*dgc5*)KO-*kan*	KAN/GEN/SB	This study
pGR008	pEX18Gm-A1S_1949(*dce2*)KO-*kan*	KAN/GEN/SB	This study
pGR009	pEX18Gm-A1S_2337(*dce1*)KO-*kan*	KAN/GEN/SB	This study
pGR010	pEX18Gm-A1S_2422(*pde1*)KO-*kan*	KAN/GEN/SB	This study
pGR011	pEX18Gm-A1S_2506(*dgc4*)KO-*kan*	KAN/GEN/SB	This study
pGR012	pEX18Gm-A1S_2986(*dgc3*)KO-*kan*	KAN/GEN/SB	This study
pGR015	pEX18Gm-A1S_3177(*pilA*)KO-*kan*	KAN/GEN/SB	This study
pGR013	pEX18Gm-A1S_3296(*dgc2*)KO-*kan*	KAN/GEN/SB	This study
pGR014	pEX18Gm-A1S_3345(*dgc1*)KO-*kan*	KAN/GEN/SB	This study
pEP382	pMMB-RIF-ABUW_0137(*dgc1*)	RIF	This study
pGR016	pMMB-RIF-ABUW_0188(*dgc2*)	RIF	This study
pGR017	pMMB-RIF-ABUW_0506(*dgc3*)	RIF	This study
pGR018	pMMB-RIF-ABUW_1045(*dgc4*)	RIF	This study
pGR019	pMMB-RIF-ABUW_1138(*pde1*)	RIF	This study
pEP434	pMMB-RIF-ABUW_1221(*dce1*)	RIF	This study
pGR020	pMMB-RIF-ABUW_1764(*dce2*)	RIF	This study
pGR021	pMMB-RIF-ABUW_2135(*dgc5*)	RIF	This study
pGR022	pMMB-RIF-ABUW_2255(*cbe1*)	RIF	This study
pGSh001	pMMB-RIF-ABUW_2824(*dgc6*)	RIF	This study
pEP380	pMMB-RIF-ABUW_3178(*dgc7*)	RIF	This study
pEP440	pMMB-RIF-ABUW_3354(*dce3*)	RIF	This study
pGR023	pMMB-RIF-A1S_1254(*pde2*)	RIF	This study

[a] RIF=rifampicin, KAN=kanamycin, GEN=gentamicin, SB=SacB, sucrose counterselection

Appendix C. Oligonucleotides Used in This Study

Primer Name [a]	Sequence	Use
pKD4 Kan Seq 5'/3'	GTC AGC ACC GTT TCT G / CGG CTG GAT CCT CC	Inside the Kan marker going for sequencing confirmation
Kan Int 5'/3' Out	CCT CTC CAC CCA AGC G / CGC CTT CTA TCG CCT TCT TG	To sequence outward from Kan resistance cassette
pEX Seq F/R	CTG CTA ACC AGT AAG GCA ACC / TAG TGA ACG GCA GGT AAG C	Within the MCS to sequence pEX suicide vector
pEX18 Gib F/R	CAT GAT CGT GCT CCT GTC GTC ACT CAA AGG CGG TAA TAC GG / GGA ATT AGC TTA CCT GCC GTT CAC TAT TAT TTA GTG	For the pEX18Gm plasmid Gibson cloning
SacB Gib F/R	CCT TTA CTA CCG CAC TGC TG / GGC TTT TGG TTC GTT TCT TTC GC	Within SacB gene to create Gibson overlaps
SacB Gib F/R #2	GGA AAC AAT GTC GTG ATT ACA AGC / GTT TGT CTG CGT AGA ATC CTC TG	Within the 3' end of SacB to create Gibson overlaps
KanR Gib F/R	GTG TAG GCT GGA GCT GCT TC / CAT ATG AAT ATC CTC CTT AG	To amplify Kan resistance marker from pKD4 for Gibson reactions
Gent Gib F/R	GGA TCG TCA CCG TAA TCT GC / GGT GCT TAT GTG ATC TAC GTG C	Within the gentamicin resistance cassette of pEX18Gm
ABUW_0137 Tn Conf	GCT GGC ACT TAC ATG AAT TTG G	To confirm Tn insertion in *dgc1*

Primer Name [a]	Sequence	Use
ABUW_0188 Tn Conf	CAG CTT GTC GCT CCA ATC G	To confirm Tn insertion in *dgc2*
ABUW_0506 Tn Conf	CTA AAT CGC ATT GCC ATG C	To confirm Tn insertion in *dgc3*
ABUW_1045 Tn Conf	GCC CAA TCG CAA TAC TAA TAG GG	To confirm Tn insertion in *dgc4*
ABUW_2135 Tn Conf	CCA CAC GCG GAT TAA ATT TCG	To confirm Tn insertion in *dgc5*
ABUW_2824 Tn Conf	GGC AAT TTC GGC GAC TTG	To confirm Tn insertion in *dgc6*
ABUW_3178 Tn Conf	GGG GGT TTC ACC GCT TAT AAT CG	To confirm Tn insertion in *dgc7*
ABUW_1138 Tn Conf	GGG TTT AGA AAT TCT TTC ACA AGC C	To confirm Tn insertion in *pde1*
ABUW_1221 Tn Conf	CTG CCT GCT CAA GCA CAA TC	To confirm Tn insertion in *dce1*
ABUW_1764 Tn Conf	GCG AAT AAC ATA TTC AGA ACC ACG	To confirm Tn insertion in *dce2*
ABUW_3354 Tn Conf	GCA ATG AGT AAA AAC TCA TCC CC	To confirm Tn insertion in *dce3*
ABUW_2255 Tn Conf	GCG AGG TGA TTC TTG CAA TTT CC	To confirm Tn insertion in *cbe1*
AB5075 *pgaA* Tn Seq	ATG ACT TGC AAA CTC GGC T	To confirm Tn insertion in *pgaA*
AB5075 *algC* Tn Seq	CGG TCA CCT CAC CAA CCA	To confirm Tn insertion in *algC*
AB5075 *csuA* Tn Seq	TAT CTT TAT AAA TTC CGG CCG CAT G	To confirm Tn insertion in *csuA*

Primer Name [a]	Sequence	Use
AB5075 *pilA* Tn Seq	ACC AGA AGC CTA ATA AGT AAA GTG AAC TTA	To confirm Tn insertion in *pilA*
A1S_3345 KO 5' Gib F/R	ACG GCA GGT AAG CTA ATT CCG CCA ACA TTA GTT CAG GTC GG / GAA GCA GCT CCA GCC TAC ACG ATG GAT GAA ATC GAG AAT CAC CTG	Delete *dgc1* from the 17978 genome
A1S_3345 KO 3' Gib F/R	CTA AGG AGG ATA TTC ATA TGG TGA TTA GAC AAG CCG ATC AAG / ACG ACA GGA GCA CGA TCA TGG AAA AAA GGG CAG TTA CAG TGG C	
A1S_3296 KO 5' Gib F/R	ACG GCA GGT AAG CTA ATT CCC AGC TTT CCC CAA GGT TGA G / GAA GCA GCT CCA GCC TAC ACC GGA ACC GCC ATA AAC AGT AAG G	Delete *dgc2* from the 17978 genome
A1S_3296 KO 3' Gib F/R	CTA AGG AGG ATA TTC ATA TGG GAG TTA TTA GAG AAC GCT GAT CG / ACG ACA GGA GCA CGA TCA TGC CTT AAC TCA GGT AGG TCT AGG C	
A1S_2986 KO 5' Gib F/R	ACG GCA GGT AAG CTA ATT CCG TTT GCT ACG AGT GGG C / GAA GCA GCT CCA GCC TAC ACT GCA TGT AGT GAA GTG GAT TG	Delete *dgc3* from the 17978 genome

Primer Name [a]	Sequence	Use
A1S_2986 KO 3' Gib F/R	CTA AGG AGG ATA TTC ATA TGG CTA AGA CTT CTG AGC AAC ATT G / ACG ACA GGA GCA CGA TCA TGG CAA CAC GAC GAT TAA TTG CC	
A1S_2506 KO 5' Gib F/R	ACG GCA GGT AAG CTA ATT CCG TGC TTA ATG AGG AAT TGT ACC C / GAA GCA GCT CCA GCC TAC ACC CAC ATT GGA ATT GGG GTG	Delete *dgc4* from the 17978 genome
A1S_2506 KO 3' Gib F/R	CTA AGG AGG ATA TTC ATA TGG TAT TGC GAT TGG GCA CG / ACG ACA GGA GCA CGA TCA TGC CAC GGC AAT ATT CCT CTT ATG	
A1S_1695 KO 5' Gib F/R	ACG GCA GGT AAG CTA ATT CCC CCA AAA CCG CTG AGA CC / GAA GCA GCT CCA GCC TAC ACC AAG TTG CTT TGG AAA CCA TAC G	Delete *dgc5* from the 17978 genome
A1S_1695 KO 3' Gib F/R	CTA AGG AGG ATA TTC ATA TGC TGC TTT TGT TAG TCG TGC TG / ACG ACA GGA GCA CGA TCA TGG CGA TGG TTT TGC TGT AGC	
A1S_1067 KO 5' Gib F/R	ACG GCA GGT AAG CTA ATT CCG CAC CAT ACG AGG GTC / GAA GCA GCT CCA GCC TAC ACC GAT GGG TAT GTA GAG TGA CC	Delete *dgc6* from the 17978 genome

Primer Name [a]	Sequence	Use
A1S_1067 KO 3' Gib F/R	CTA AGG AGG ATA TTC ATA TGC AGC CAT TAC AAG TCG CTG / ACG ACA GGA GCA CGA TCA TGG TTG GTT CGA CTC ACA AGC	
A1S_0751 KO 5' Gib F/R	ACG GCA GGT AAG CTA ATT CCG GAT AAC TCC TGG CAG GC / GAA GCA GCT CCA GCC TAC ACG AGG ACG AGA TGC AAT TCC	Delete *dgc7* from the 17978 genome
A1S_0751 KO 3' Gib F/R	CTA AGG AGG ATA TTC ATA TGC TCC AAG CTA TCA CCG TTC / ACG ACA GGA GCA CGA TCA TGG GCT GAT CCC CAT TCA AAG TC	
A1S_2422 KO 5' Gib F/R	ACG GCA GGT AAG CTA ATT CCG CGT GGC GGT GTA ATT CG / GAA GCA GCT CCA GCC TAC ACG AGT TTC TCA CTT TAA TGC TTC CC	Delete *pde1* from the 17978 genome
A1S_2422 KO 3' Gib F/R	CTA AGG AGG ATA TTC ATA TGC GCT TAA CAG ACG TAC AAG ACC / ACG ACA GGA GCA CGA TCA TGG GCG TAT AAT ACT GCC CAC TTG	
A1S_1254 KO 5' Gib F/R	ACG GCA GGT AAG CTA ATT CCG GCT GTA CCT GAG AGT CAT AG / GAA GCA GCT CCA GCC TAC ACG TAT CCC TGC CGA AAT ACG	Delete *pde2* from the 17978 genome

Primer Name [a]	Sequence	Use
A1S_1254 KO 3' Gib F/R	CTA AGG AGG ATA TTC ATA TGG TTG TAC CGA GTT TCA GGG / ACG ACA GGA GCA CGA TCA TGC CTT GGC TTC AAT TTG TTC AGA TG	
A1S_2337 KO 5' Gib F/R	ACG GCA GGT AAG CTA ATT CCG TTC CAG AAG TTT TAG CCC C / GAA GCA GCT CCA GCC TAC ACG CGG ATA TAT TGA ATT GAG AGG C	Delete *dce1* from the 17978 genome
A1S_2337 KO 3' Gib F/R	CTA AGG AGG ATA TTC ATA TGG CCG TCC ACT TCA TCC / ACG ACA GGA GCA CGA TCA TGG AGC AGC AAC CCC TG	
A1S_1949 KO 5' Gib F/R	ACG GCA GGT AAG CTA ATT CCG GAA ACC GTA TAA AAA GCC TCC / GAA GCA GCT CCA GCC TAC ACG GGT AGT GTT CGA CAT TGA AG	Delete *dce2* from the 17978 genome
A1S_1949 KO 3' Gib F/R	CTA AGG AGG ATA TTC ATA TGG TAT TCT TAA ACA GGG TCA GGC / ACG ACA GGA GCA CGA TCA TGC CTT TTC GCC CAT GAG AAC C	
A1S_0546 KO 5' Gib F/R	ACG GCA GGT AAG CTA ATT CCC TGG TGC TAA ATT ACG TGC G / GAA GCA GCT CCA GCC TAC ACG CAA TAA AAG AGC CGA CGA TC	Delete *dce3* from the 17978 genome

Primer Name [a]	Sequence	Use
A1S_0546 KO 3' Gib F/R	CTA AGG AGG ATA TTC ATA TGC AGT CGC AAG GTG CTC / ACG ACA GGA GCA CGA TCA TGG TGA AGA ACT GAC GCC TG	
A1S_1559 KO 5' Gib F/R	ACG GCA GGT AAG CTA ATT CCC ATT TAG CGG AAA CAG CAT CAG / GAA GCA GCT CCA GCC TAC ACG ACC TGA ATA ATT CCA CCC ATT TG	Delete *cbe1* from the 17978 genome
A1S_1559 KO 3' Gib F/R	CTA AGG AGG ATA TTC ATA TGG GTA GTA TGT CTT TAG ATC GCC C / ACG ACA GGA GCA CGA TCA TGC CAC CGT ATC ATG TTT TGC TG	
A1S_0490 KO 5' Gib F/R	ACG GCA GGT AAG CTA ATT CCG CCG CCA AGA TAG CTG C / GAA GCA GCT CCA GCC TAC ACC ATG TGG TAC GAG CTG GC	Delete *cbe2* from the 17978 genome
A1S_0490 KO 3' Gib F/R	CTA AGG AGG ATA TTC ATA TGC CAG AAA CAA GCA GCT TAA CG / ACG ACA GGA GCA CGA TCA TGG TTT GAC TCT AAC CGC CCA C	
17978 *pilA* KO 5' Gib F/R	ACG GCA GGT AAG CTA ATT CCC GAT TGT AGA GCA GCT TCA AC / GAA GCA GCT CCA GCC TAC ACC CGA TAA TGG CAA CCA CGA TC	Delete *pilA* from the 17978 genome

Primer Name [a]	Sequence	Use
17978 *pilA* KO 3' Gib F/R	CTA AGG ATA TTC ATA TGC AGT AAT TGC TCC AAA AGG CTG / ACG ACA GGA GCA CGA TCA TGC CAA CAG CTA CCG TCA ATA CC	
A1S_3345 KO Conf F/R	CAT ATT GCG GCA GAT GAC C / CTT AGT TTA TTG CTA GGG CTG GC	Flanking *dgc1* in 17978 to confirm deletion
A1S_3296 KO Conf F/R	GTG CTT TCC CAG ATA CGA TGT G / GCT ATT CCA GTT ATT CAC CGT CG	Flanking *dgc2* in 17978 to confirm deletion
A1S_2986 KO Conf F/R	CTC ACC ATG TGG CAC TCC / CCA TTA AGA TTT CGT GTA CCG CC	Flanking *dgc3* in 17978 to confirm deletion
A1S_2506 KO Conf F/R	CAC AGT TCC CAA CAC TCA CTC / GGA CGG TTT GAT AGC ATT GAC	Flanking *dgc4* in 17978 to confirm deletion
A1S_1695 KO Conf F/R	CAC CCG CTC CTT AAC TGG / CAA TGC GGT TAA GGG TGT TG	Flanking *dgc5* in 17978 to confirm deletion
A1S_1067 KO Conf F/R	CAT CTG GTG AAG TGT GGT CAG / CGA GCG TTT GCT TAC TGG	Flanking *dgc6* in 17978 to confirm deletion
A1S_0751 KO Conf F/R	GGA GTA AGG GAA CTG TGA GC / CTT CTC AGG CTA TTG AGT GC	Flanking *dgc7* in 17978 to confirm deletion
A1S_2422 KO Conf F/R	GGT GAA GGA AAC GCT ACA TGG / GGT CTG TGG GGT CAT TGC	Flanking *pde1* in 17978 to confirm deletion

Primer Name [a]	Sequence	Use
A1S_1254 KO Conf F/R	CTC ACA ACT TGG TCA TTA GCA GC / CCA ATC ATC GTA TCG GTA AA ACC	Flanking *pde2* in 17978 to confirm deletion
A1S_2337 KO Conf F/R	CAG CAT GTG AGC AAT GTG G / GCT GAA GGA TCA CGT TCA ATC	Flanking *dce1* in 17978 to confirm deletion
A1S_1949 KO Conf F/R	CCG TCA ATG GTG GGT ACT TG / CGA CCA ATA CTG GCA CAT G	Flanking *dce2* in 17978 to confirm deletion
A1S_0546 KO Conf F/R	GAC AGC TCG TCG TCG TC / CTG CCC TAA CGC ATC TCA AG	Flanking *dce3* in 17978 to confirm deletion
A1S_1559 KO Conf F/R	GAG CCA GGT GAA CGC / AAT ACC ATG TGT AGA TTG TTC AGC TCG	Flanking *cbe1* in 17978 to confirm deletion
A1S_0490 KO Conf F/R	GCT CAA GAC GAT CAA GTA AGG C / CAG TCG ATT TAT TTA CCG AAG CC	Flanking *cbe2* in 17978 to confirm deletion
A1S_3177 KO Conf F/R	GAT CGT GGG ATT AGG AGT GC / GTT GAC CAA AGT TGC CGT AAG	Flanking *pilA* in 17978 to confirm deletion
pMMB Seq F	ATG TGT GGA ATT GTG AGC GG	Inserts in pMMB vector to confirm with R Comp primers
pMMB Gib F/R #1	CAT GCC GGA GTT CGT CG / GCG TTC ATA CAG GTC GGC	To amplify pMMB backbone fragments for Gibson reactions
pMMB Gib F/R #2	CGA TAC CGG GTG CTC TAT CG / CCT GCG CCC ATC ATG G	

Primer Name [a]	Sequence	Use
pMMB #2 Gib F/R #1	GCA TGG AGC CGA AAA GC / CAT GCT GCC TCG CTG TTG	Improve efficiency within pMMB backbone for Gibson reactions
pMMB #2 Gib F/R #2	GCA GCT CGG TAC TGG TC / TAG GAC TGC CAG CGG ATG	
Ptac MCS Gib R	CGA ATT CTG TTT CCT GTG TGA AAT TG	Amplify through the Ptac promoter to create a pMMB fragment for Gibson reactions
rrnB Term Gib F	GGC TGT TTT GGC GGA TGA GAG AAG	Amplify after the MCS for pMMB fragment Gibson reactions
ABUW_0137 Comp Gib F/R	ATA TTA GAA TTC ATG AAA ATT CGT TTA ATC ACT CGT CC / ATA TTA CTG CAG GAT TCA AAT TGA TTT GAT CTG AGG TAG	To Gibson clone *dgc1* into pMMB-RIF
ABUW_0188 Comp Gib F/R	ATA ACA ATT TCA CAC AGG AAA CAG AAT TCG ATG TCA GGA TTA CGT TCA GAA C / GAA AAT CTT CTC TCA TCC GCC AAA ACA GCC TTA TCC CTC TAC TAC ATT CCG TCC C	To Gibson clone *dgc2* into pMMB-RIF
ABUW_0506 Comp Gib F/R	ATA ACA ATT TCA CAC AGG AAA CAG AAT TCG ATG ATA TCT AAG TTG TAT CAA TCC ACT TCG / GAA AAT CTT CTC TCA TCC GCC AAA ACA GCC GCA ATG CAA TAA AGG AGA GTT TCA	To Gibson clone *dgc3* into pMMB-RIF

Primer Name [a]	Sequence	Use
ABUW_1045 Comp Gib F/R	ATA ACA ATT TCA CAC AGG AAA CAG AAT TCG ATG GAA ACT TTA GAT TCT TCA ATT TTT GAC / GAA AAT CTT CTC TCA TCC GCC AAA ACA GCC CTC GTC GTT CTA TGG GTA AGC	To Gibson clone *dgc4* into pMMB-RIF
ABUW_2135 Comp Gib F/R	ATA ACA ATT TCA CAC AGG AAA CAG AAT TCG ATG AAG TTG CAG GGT TCC AAT ATA T / GAA AAT CTT CTC TCA TCC GCC AAA ACA GCC GTT CTA ATC AGC GTA TTT AAA AAG CCA C	To Gibson clone *dgc5* into pMMB-RIF
ABUW_2824 Comp Gib F/R	ATA ACA ATT TCA CAC AGG AAA CAG AAT TCG GTG GCG AAT AGG GGA AAT GTA C / GAA AAT CTT CTC TCA TCC GCC AAA ACA GCC GTT AGG CAA TTT CGG CGA CTT G	To Gibson clone *dgc6* into pMMB-RIF
ABUW_3178 Comp Gib F/R	ATA TTA GAG CTC ATG CCA TAC TCA CTT CGT GAA / ATA TTA AAG CTT GAC TTG GAA ATA TTA CAA AGA AAT AAA AAC TC	To Gibson clone *dgc7* into pMMB-RIF

Primer Name [a]	Sequence	Use
ABUW_1138 Comp Gib F/R	ATA ACA ATT TCA CAC AGG AAA CAG AAT TCG ATG GGA AGC ATT AAA GTG AGA AAC / GAA AAT CTT CTC TCA TCC GCC AAA ACA GCC CAA AAC GAA ACA AAA AAC GGG C	To Gibson clone *pde1* into pMMB-RIF
A1S_1254 Comp Gib F/R	ATA ACA ATT TCA CAC AGG AAA CAG AAT TCG ATG TGG GTG ATT GTT TAT ATG GAT ATC TG / GAA AAT CTT CTC TCA TCC GCC AAA ACA GCC TTA TTC TTT ATC GAT CTT GAT GGG C	To Gibson clone *pde2* into pMMB-RIF
ABUW_1221 Comp Gib F/R	ATA TTA GAA TTC ATG TCT GGC CTT CAG GAA GA / ATA TTA CTG CAG TTA AAA CAA TTA TCA AAT ATG CGT ATT TGT TTG	To Gibson clone *dce1* into pMMB-RIF
ABUW_1764 Comp Gib F/R	ATA ACA ATT TCA CAC AGG AAA CAG AAT TCG ATG ACT TCA ATG TCG AAC ACT ACC / GAA AAT CTT CTC TCA TCC GCC AAA ACA GCC CTT GTT ATC GTT ATG GTT ATA TTA TCG CC	To Gibson clone *dce2* into pMMB-RIF
ABUW_3354 Comp Gib F/R	ATA TTA GAA TTC ATG GGT CAT GTT GAT TAC GAT AGC ACA T / ATA TTA CTG CAG GAC AAC CGG CTG GCA ATG TAG G	To Gibson clone *dce3* into pMMB-RIF

Primer Name [a]	Sequence	Use
ABUW_2255 Comp Gib F/R	ATA ACA ATT TCA CAC AGG AAA CAG AAT TCG ATG CAA CCA CAA ATG GGT G / GAA AAT CTT CTC TCA TCC GCC AAA ACA GCC TTA CAT GGT ATA ACT TGG GCG ATC	To Gibson clone *cbe1* into pMMB-RIF
A1S_0490 Comp Gib F/R	ATA ACA ATT TCA CAC AGG AAA CAG AAT TCG ATG AAT TCC AT TATT CAA ATG GAT TCG G/ GAA ATT CTT CTC TCA TCC GCC AA ACA GCC TTA AGC TGC TTG TTT CTG GCG	To Gibson clone *cbe2* into pMMB-RIF
PA2133 Comp Gib F/R	ATA TTA GAA TTC GTG AAC GGT TCC CCA CAG / ATA TTA AAG CTT CAG ATT TTT CGC CGA CCG TG	To Gibson clone PA2133 (PDE) into pMMB-RIF
PA3702 Comp Gib F/R	ATA TTA GAA TTC ATG CAC AAC CCT CAT GAG AGC / ATA TTA AAG CTT CCC ACA GGC AGT ACG C	To Gibson clone PA3702 (DGC) into pMMB-RIF

[a] Use of abbreviations in the primer names were used for convenience and to save space. *F* and *R* stand for *forward* and *reverse*, respectively. *Comp* stands for *Complement*. *Gib* stands for *Gibson*. *KO* stands for *knockout*. *Seq* and *Conf* stand for *sequence* and *confirmation*, respectively. *Int* stands for *interior*. *Tn* stands for *transposon*.

Appendix D. AB5075 and 17978 Homologues

Gene	AB5075 Gene Number	17978 Gene Number
dgc1	ABUW_0137	A1S_3345
dgc2	ABUW_0188	A1S_3296
dgc3	ABUW_0506	A1S_2986
dgc4	ABUW_1045	A1S_2506
dgc5	ABUW_2135	A1S_1695
dgc6	ABUW_2824	A1S_1067
dgc7	ABUW_3178	A1S_0751
pde1	ABUW_1138	A1S_2422
pde2	ABUW_2631 [ab]	A1S_1254
dce1	ABUW_1221	A1S_2337
dce2	ABUW_1764	A1S_1949
dce3	ABUW_3354	A1S_0546
cbe1	ABUW_2255	A1S_1559
cbe2	ABUW_3388 [b]	A1S_0490
pgaA	ABUW_1557	A1S_2162 [b]
algC	ABUW_3041	A1S_0887 [bc]
csuA	ABUW_1488	A1S_2217 [b]
pilA	ABUW_0304	A1S_3177

[a] ABUW_2631, aka *pde2*, is a pseudogene in AB5075.

[b] Not included in this study.

[c] KEGG GENOME database returns two genes that encode phosphomannomutase, the first being A1S_0887 and the second being A1S_0066. Although, A1S_0066 is considered to code for a hypothetical phosphomannomutase protein, whereas A1S_0887 is considered to code for phosphomannomutase / phosphoglucomutase.

Appendix E. *Acinetobacter baumannii* 17978

Originally named *Moraxella glucidolytica* subspecies *nonliquefaciens*, *A. baumannii* strain ATCC® 17978™ is a clinical isolate from 1951 (99). The strain was from a four-month-old infant patient with fatal meningitis in France. It contains a genome with almost four million nucleotides and two plasmids with, on average, 12,000 bases (100). *A. baumannii* 17978 is a type strain susceptible to many antibiotics and retains many phenotypic traits of *A. baumannii* relatives. Though it differs slightly from more recent isolates, it remains a highly studied strain with similar systems (e.g., biofilm production, type II secretion systems, iron-acquisition systems) comparable to many other *A. baumannii* strains.

A. baumannii 17978 Surface Motility

A. baumannii 17978 is not capable of twitching along plastic surfaces as its AB5075 relative is. Conversely, 17978 moves along a semi-solid agar surface in a manner like swarming, although swarming should only be done by bacteria with rotating flagella (101). Neither *A. baumannii* AB5075 nor 17978 have flagella, making the presence of swarming in 17978 unconventional. Genes encoding each of the 12 CMEs of *A. baumannii* 17978 along with two genes encoding CBE proteins were deleted through homologous recombination of a suicide vector (97). These strains were tested for their ability to exhibit the surface motility seen in *A. baumannii* 17978. Included with these strains were also two positive controls with either a DGC or PDE incorporated into pMMB-RIF to compare results during the complement tests to see if induction of these *P. aeruginosa* known-CMEs were similar to the expression of the *A. baumannii* CMEs.

17978 exhibits surface-associated motility by translocating along a semisolid surface, sometimes referred to as ‘sliding’ or ‘gliding’ (102). One potential mechanism for this flagellar-independent surface motility could be similar to the *P. aeruginosa* flagellum- and pilus-independent motility due to the postulated rhamnolipid surfactant production (103). The physical mechanism behind surface motility in 17978 is not understood. Surface motility in *A. baumannii* has been previously determined to be regulated by quorum sensing (81-83), light (84, 85), iron availability (86), surfactant-like compounds (81, 104), lipooligosaccharide presence (105), diaminopimelic acid (106), and recently, c-di-GMP (47). While the mechanism of bacterial surface translocation in *A. baumannii* is not currently understood, the lack of flagellar genes precludes that option.

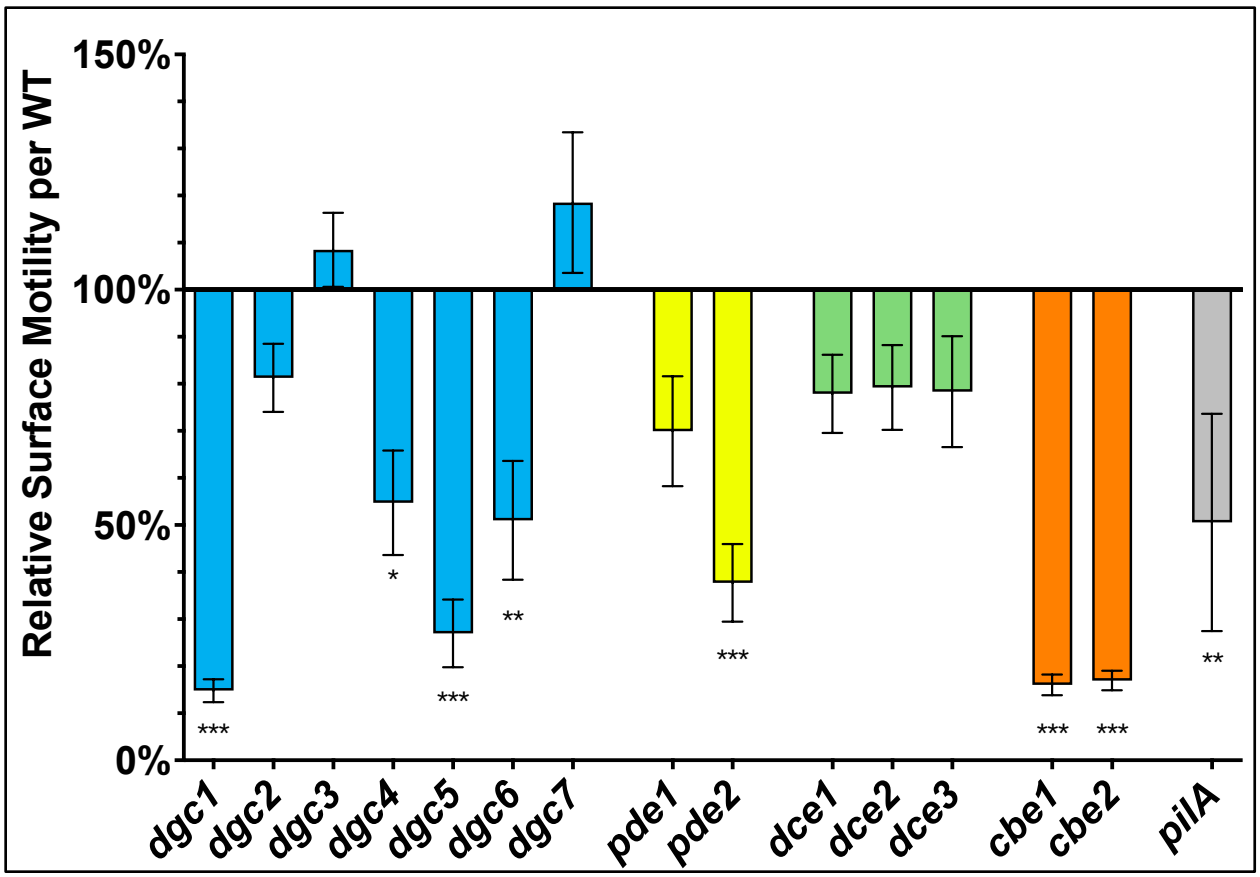

Appendix E1. Deletions of CME genes *dgc1*, *dgc4*, *dgc5*, *dgc6*, *pde2*, *cbe1*, and *cbe2* all alter surface motility in *A. baumannii* 17978

Overnight cultures of above deletion mutants were inoculated onto the center of a 0.4 % agar plate containing 5.0 g/L tryptone and 2.5 g/L NaCl and incubated overnight at 37 °C. Perpendicular diameters of the motility regions were measured and compared to wild-type 17978 using ANOVA with Dunnett's post hoc test. Shown is the relative change in distance traveled of each strain (± SEM) versus the WT (at 100 %). n=5. * = $p<0.05$, ** = $p<0.01$, *** = $p<0.001$

Both putative CBEs (*cbe1* and *cbe2*) are required for surface motility, according to original testing (Appendix E1). Like twitching motility, this could be due to c-di-GMP interactions (67), loss of the proteins causing the destabilization of the pili (70), or other potential mechanism of this surface motility (102, 107). A *pilA* mutant showed decreased but variable surface motility, suggesting that the pilus may play a role. Deletion of *pde2*, the pseudogenized phosphodiesterase in AB5075, also significantly reduced 17978 surface motility and successfully complemented. The DGC-encoding genes—*dgc1*, *dgc4*, *dgc5*, and *dgc6*—and the CBE gene, *cbe1*, were significantly reduced compared to the wild-type strain during the original testing, but unfortunately, these clones did not return to wild type when complementing (Appendix E2). Future work will be required to determine if these were properly expressed in these strains, or if these mutants contain a secondary mutation to the identified deletion.

A. baumannii 17978 Biofilm Formation

No significantly different phenotype from wild-type 17978 was seen in any mutant during the biofilm formation assays in LB (Appendix E3), low-salt LB, and Mueller–Hinton broth (data not shown). Redundancy was also found when expressing a DGC and a PDE in the wild-type 17978 strain, which hardly altered biofilm levels (Appendix E3). A previous study has shown that overexpression of *dgc2*, *dgc4*, and *dce2* in *A. baumannii* 17978 does result in a detectable change in biofilm levels (47). Notably, they suspended their bacterial cells grown overnight on LB agar plates in PBS at 1.0 OD_{600} and diluted by ten when transferring to their 96-well plates in LB with 100 µg/mL carbenicillin. The other group's 1 % crystal violet was dissolved in 5 % acetic acid rather than 95 % ethanol. My wild-type 17978 crystal violet stained raw OD_{595} values were

consistently around 2.500 OD_{595}. Their results show that there is up to a +300 % increase in the *dgc4* mutant per wild type, which would be 10.000 OD_{595} based on my wild-type OD_{595} values. That value is undetectable by 96-well plate readers, so there seems to be some discrepancy between the strains, a variable within either protocol, or a difference in laboratory machinery (i.e., 96-well plate reader) that is affecting these results. Even overexpression of the DGC_{PA3702} showed an insignificant increase in my study. One other possibility is that c-di-GMP levels may be relatively high in wild-type 17978 such that deletion of a single DGC fails to reduce c-di-GMP below the level required for biofilm formation.

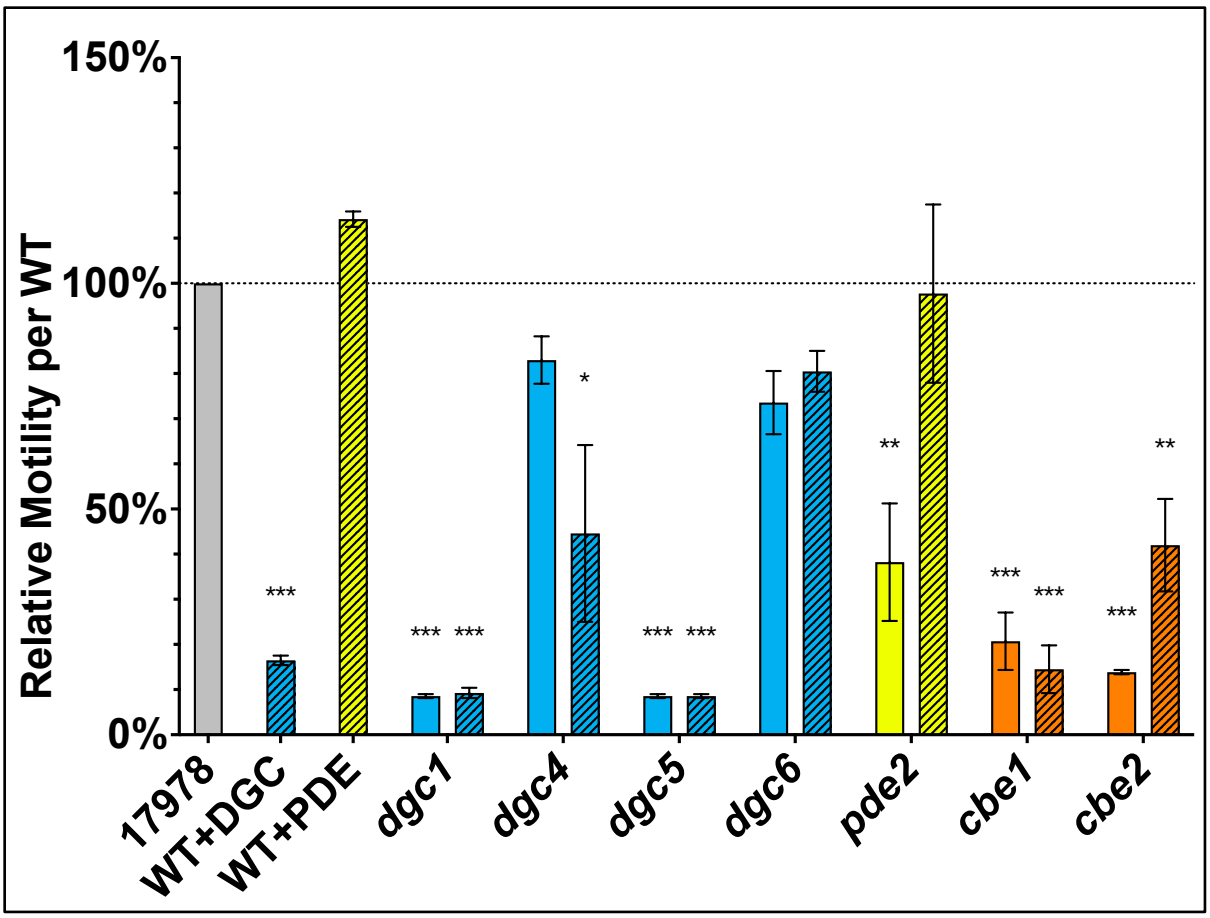

Appendix E2. Only *pde2* complemented the wild-type surface motility phenotype in *A. baumannii* 17978

Overnight cultures of above complemented 17978 mutants were inoculated onto the center of a 0.4 % agar plate containing 5.0 g/L tryptone, 2.5 g/L NaCl, and 1 mM IPTG and then incubated overnight at 37 °C. Perpendicular diameters of the motility regions were measured and compared to 17978 WT+pEV using ANOVA with Dunnett's post hoc test. Shown is the relative change in distance traveled of each strain (± SEM) versus the WT+pEV (at 100 %). n=3. * = $p<0.05$, ** = $p<0.01$, *** = $p<0.001$

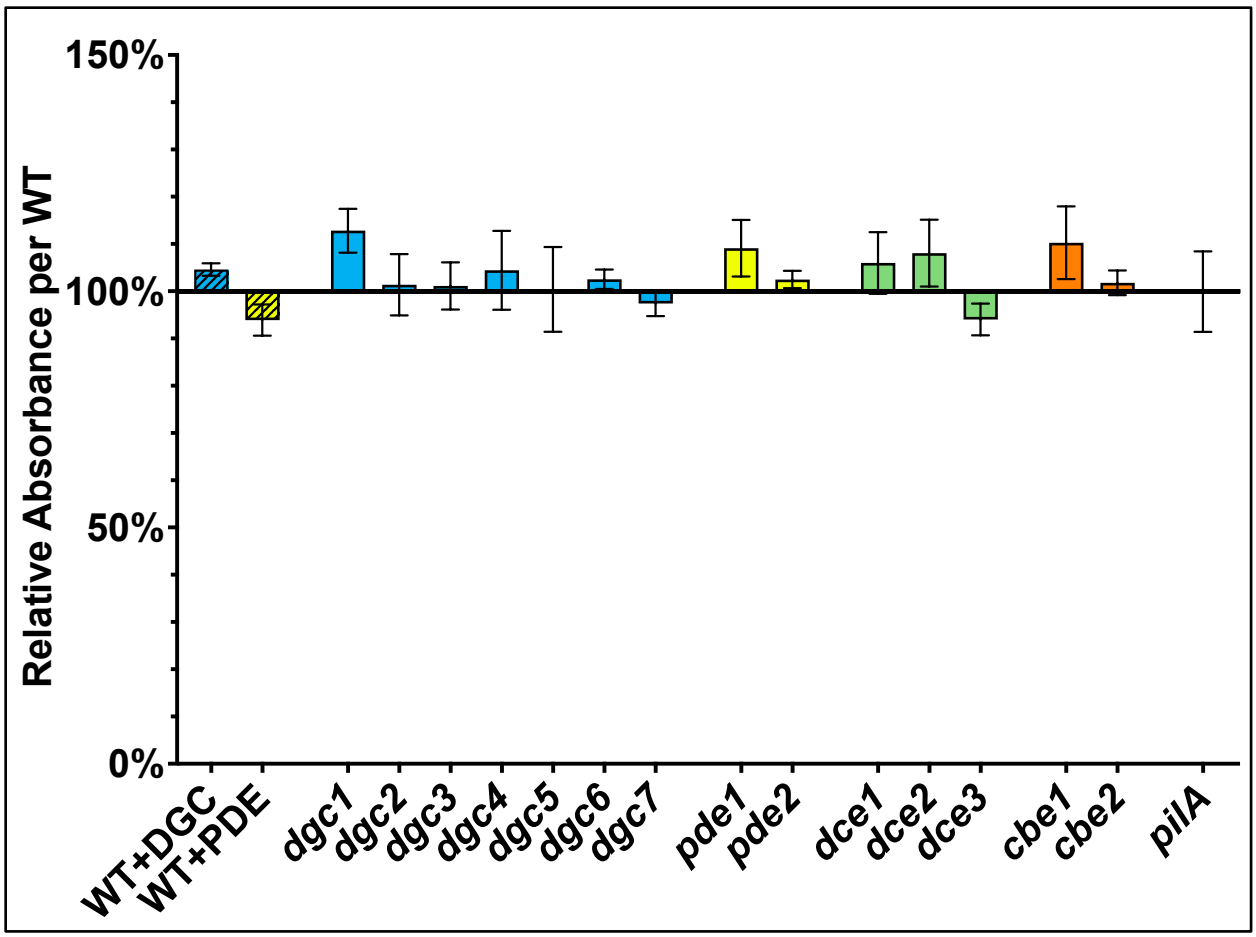

Appendix E3. No CME deletions in 17978 affected biofilm formation

Overnight cultures of above deletion mutants were diluted to 0.05 OD_{600} and grown in LB overnight at 37 °C in 96-well plates. The 96-well plates were then washed in distilled water, stained with 0.1 % crystal violet, and quantified by dissolving the adhered crystal violet dye with 95 % ethanol. The OD_{595} of the released crystal violet was measured and compared to wild-type 17978 using ANOVA with Dunnett's post hoc test. Shown is the relative change of the measured OD_{595} of each strain (± SEM) versus the wild type (at 100 %). n=3

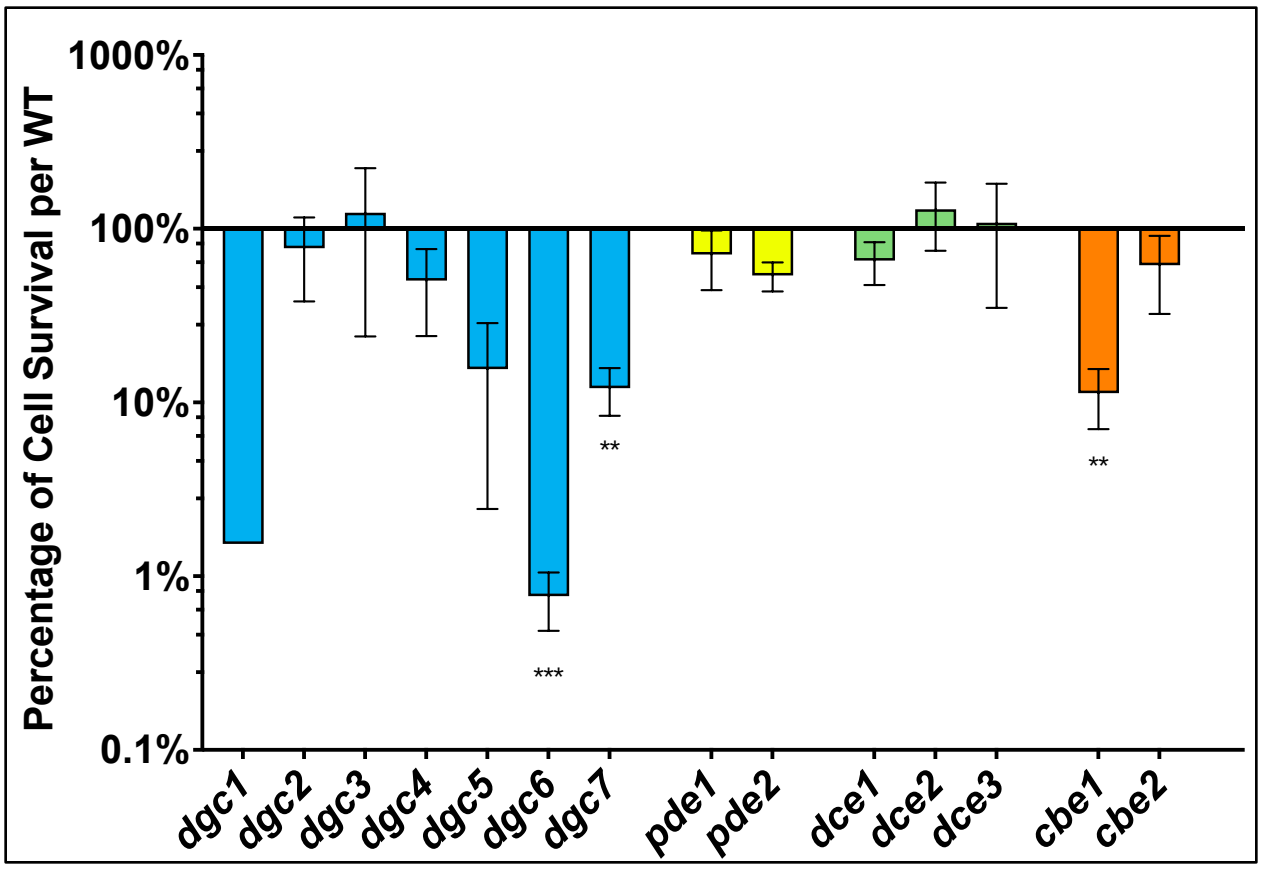

Appendix E4. Deletions of genes *dgc6*, *dgc7*, and *cbe1* determined survival after 48-hour exposure to a desiccating environment in *A. baumannii* 17978

Overnight cultures of above deletion mutants were washed and diluted with distilled water. One 96-well plate was dried 48 hours, and a separate 96-well plate was used to serially dilute cultures to a countable number of colonies. After 48 hours, the same was done to the dried 96-well plate. Colony-forming units were converted to CFU/mL to compare mutants to the wild-type value. ANOVA with Dunnett's post hoc test was used to determine statistical significance against wild type. Shown is the percentage of cell survival per wild type (± SEM) and is defined as the CFU/mL of mutants divided by the CFU/mL of wild-type 17978 (at 100 %). n=3. ** = $p<0.01$, *** = $p<0.001$

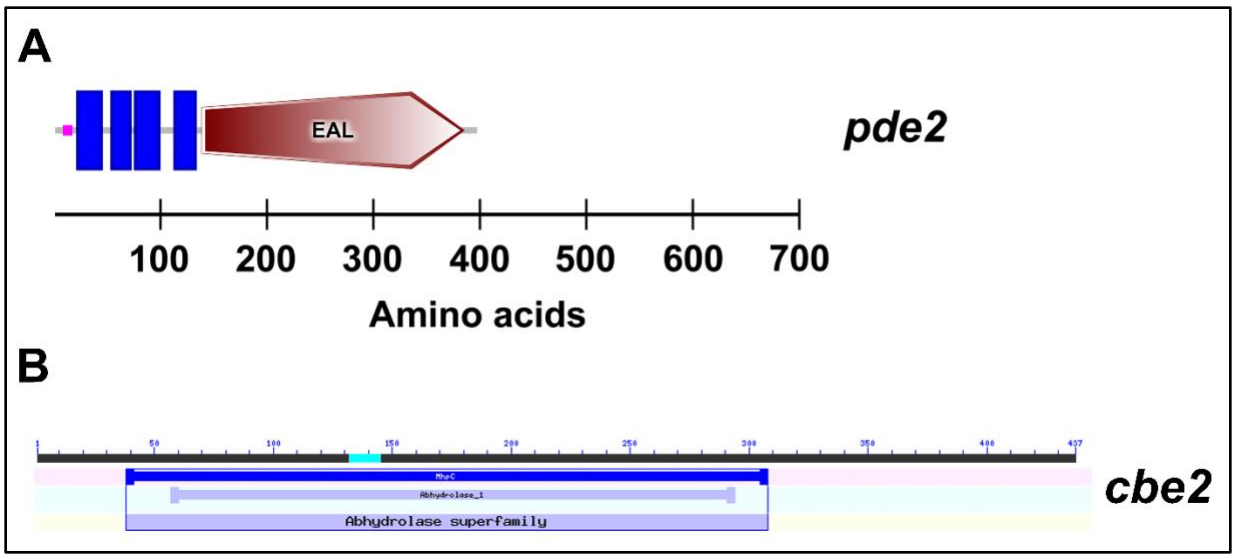

Appendix E5. *A. baumannii* 17978 codes for an additional PDE and CBE

Using the Conserved Domain Database, a putative diguanylate PDE is shown above. A putative c-di-GMP–binding effector is also seen in the *A. baumannii* 17978 genome. Gene "*pde2*" is likely a pseudogene in AB5075 from a frameshift mutation by deletion; thus, coding for a protein starting at the 129th residue. Gene "*cbe2*" contains a hydrolase domain on its N-terminus and a potential c-di-GMP–binding site on its C-terminus.

Generation of 17978 Deletion Mutants

A. baumannii 17978 mutants were generated by double homologous recombination using the pEXGm18 suicide vector. Purified genomic DNA (MasterPure™ Complete DNA and RNA Purification Kit) was used as template DNA in a PCR reaction to amplify regions neighboring the gene of interest (5' KO and 3' KO). The neighboring regions were inserted using Gibson cloning into pEXGm18, flanking a kanamycin resistance cassette. This vector also contains a gentamicin resistance cassette and *sacB* counterselection gene, so confirmation of vector identity was done

by PCR, ensuring the expression vector contained *sacB*, Kan^R cassette, Gen^R cassette, and the KO gene fragments. Vectors were electroporated into 17978, and vector-integrated strains were selected on LB with 50 µg/mL KAN agar plates. Strains containing the deletion suicide vector were grown overnight in LB with 50 µg/mL KAN medium and were then struck out onto LB agar plates with 50 µg/mL KAN and 6 % sucrose to select for colonies that had lost the *sacB* gene. Death occurs by *sacB* encoded levansucrase which may convert sucrose to levans, toxifying itself from levan accumulation in the periplasm of Gram-negative bacteria (108). Counterselection was confirmed by testing for loss of gentamicin resistance on LB agar plates with 30 µg/mL GEN. A colony PCR with Kan^R, Gen^R, *sacB* and KO 5' and 3' primers was done to confirm deletion. Correct mutants showed presence of Kan^R and the corresponding 5' and 3' fragment as well as a change in the size between the 5' and 3' fragments; they also showed no presence of *sacB* and Gen^R cassette.

Generation of 17978 Complement Mutants

Complementation for *A. baumannii* 17978 mutants were made by electroporating *A. baumannii* AB5075 homologues into the corresponding 17978 strains. The homology between the genes were almost an identical match, while sometimes showing a single silent mutation. Inserted genes were previously sequenced to confirm integrity. The complement vector and empty vector control were electroporated into the proper 17978 strains. Replication in the 17978 mutant strains was confirmed by standard PCR with primers within the gene of interest.

A. baumannii 17978 Surface Motility Assay Method

Surface motility plates were made from a modified LB recipe containing 5.0 g/L Fisher BioReagents™ tryptone, 2.5 g/L Fisher BioReagents™ NaCl, and 4.0 g/L powdered Fisher Science Education™ Agar Bacteriological. Surface assay motility plates were made the day prior to experimentation, dried overnight, and used the following day. Bacterial cultures were grown in 2 mL LB medium 20–24 hours to stationary phase. Overnight cultures were diluted to 1.0 OD_{600} in 1 mL LB, and 2 µL each sample were dropped onto the agar surface (Appendix E6). Plates were incubated 20–24 hours at 37 °C. The diameter of the distance traveled was measured in two directions perpendicular to one another. Average diameters were calculated, and normalized values were computed relative to the wild type. The assay was repeated in quadruplicate, and the results were analyzed by ANOVA with Dunnett's post hoc test (against a control: wild type) for statistical significance ($p<0.05$) using GraphPad Prism v9.4.0. When necessary, complementation tests had 1 mM IPTG included in the medium to induce the expression of the pMMB-RIF vector.

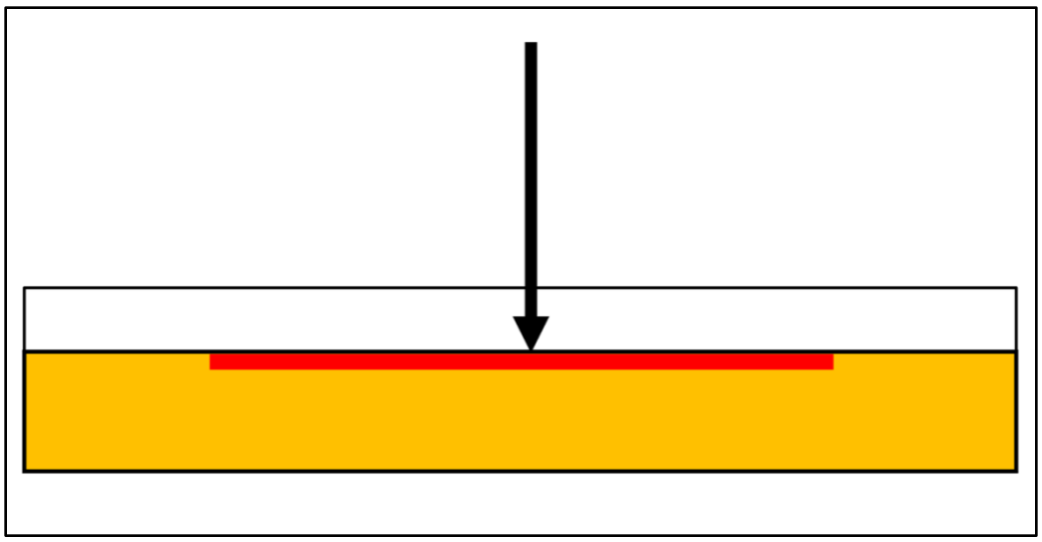

Appendix E6. Surface motility plate inoculation technique

The above picture shows a standard Petri dish; the smaller (top) rectangle is the lid of the dish. The yellow represents the motility medium containing 5.0 g/L Fisher BioReagents™ tryptone, 2.5 g/L Fisher BioReagents™ NaCl, and 4.0 g/L powdered Fisher Science Education™ Agar Bacteriological. The red represents the area the bacteria will grow. The black arrow shows the way the bacteria were inoculated onto the medium by passing the opened lid and to the top of the medium. 2 µL of 1.0 OD_{600} AB5075 transposon mutant cultures were dropped onto the plate (black arrow) and grown 20–24 hours at 37 °C. The bacteria grew (red) on top of the motility medium (yellow). Perpendicular diameters of bacterial growth (red) were measured and averaged.

VITA

GARRETT REYNOLDS

Education:	M.S. Biology-Microbiology Concentration, East Tennessee State University, Johnson City, Tennessee 2022
	B.S. Microbiology, ETSU, Johnson City, Tennessee, 2020
	B.S. Chemistry-Chemistry Concentration, ETSU, Johnson City, Tennessee, 2020
Professional Experience:	Graduate Assistant, ETSU, College of Public Health, 2020–2022
	Graduate Researcher, ETSU, Johnson City, Tennessee, 2020–2022
	Professional Tutor, Independent, Tennessee, 2017–2022
Presentations:	Cyclic Di-GMP Regulates Biofilm Formation, Desiccation Tolerance, and Motility in *Acinetobacter baumannii* (2022). Appalachian Student Research Forum.
	An investigation of cyclic di-GMP's role in motility, desiccation tolerance, and biofilm-producing phenotypes in *Acinetobacter baumannii* (2021). ETSU Biology Seminar.
Honors and Awards:	Graduate Assistantship, ETSU, 2020–2022
	Appalachian Student Research Forum First Prize in Master's Student of Public Health, ETSU, 2022